Progress in Oceanography 178 (2019) 102160

Contents lists available at ScienceDirect

Progress in Oceanography

journal homepage: www.elsevier.com/locate/pocean

One new genus and two new free-living deep-sea nematode species with discussion of phylogeny of the family Leptosomatidae Filipjev, 1916

Vladimir V. Mordukhovich[a,b,*], Alexandr A. Semenchenko[a], Natalya P. Fadeeva[a], Julia K. Zograf[b]

[a] Far Eastern Federal University, 27 Oktyabrskaya St., Vladivostok 690091, Russia
[b] A.V. Zhirmunsky National Scientific Centre of Marine Biology FEB RAS, 17 Paltchevsky St., Vladivostok 690041, Russia

ARTICLE INFO

Keywords:
Free-living nematodes
Kurile-Kamchatka Trench
Leptosomatidae
DNA barcoding
Phylogenetic relationships
Scanning electron microscopy
CLCM

ABSTRACT

Two nematode species of the subfamily Synonchinae Platonova, 1970, (Leptosomatidae Filipjev, 1916) were isolated during deep-sea expeditions to the Kurile-Kamchatka Trench and adjacent area, for morphological and molecular analyses. One new genus and two new species are described. *Platonova* gen. nov. differs from other known Synonchinae genera by the tail shape, by the pronounced division of pharyngostome into 2 parts, by the presence of one dorsal tooth in the anterior part of pharyngostome, by the presence of cuticular beams and microonchia in the posterior part of pharyngostome. *Platonova magna* sp.nov. is characterised by the combination of following characters: very large body size, cheilostome with three mandibular ridge, posterior part of pharyngostome with 6 cuticular beams 43–51 μm long, two ventrosublateral microonchia at about the level of the middle of the cuticular beams and dorsal microonchium at the base of cuticular beams, one ventral pre-cloacal supplement, spicules 214–243 μm, with wide vellum, capitulum with incision ending in circular fenestra. *Platonova verecunda* sp nov. is characterised by the combination of following characters: very large body size, cheilostome with three mandibular ridges, posterior part of pharyngostome with 6 cuticular beams 19–27 μm long, two ventrosublateral microonchia at the level of apical part of the cuticular beams and dorsal microonchium at the base of cuticular beams, one ventral pre-cloacal supplement, spicules 152–161 μm, with wide vellum, capitulum with circular fenestra. BI and ML phylogenetic analysis based on 18S and 28S rDNA suggest that Leptosomatidae requires transfer from superfamily Ironoidea (suborder Ironina) to superfamily Enoploidea (suborder Enoplina). Phylogenetic relationships within the family Leptosomatidae remained unresolved despite of the various sequences analysed in different loci. Finally, spatial distribution of the described species was analyzed.

1. Introduction

Nematodes are usually encountered in macrofauna communities, and they often dominate in numbers and are characterized by high species richness (Brandt et al., 2015; Gunton et al., 2017; Sharma et al., 2011). However, knowledge of macrobenthic nematodes remains rather limited, and they are often identified only at the phylum level and not considered in macrobenthic assemblages. A typical representative deep-sea macrobenthic nematodes with a high abundance and frequency of occurrence are leptosomatids. Some species of this family are the largest free-living nematodes, and their body length can reach up to 50 mm (Tchesunov, 2006). Describing and identifying the nematode species from this family are often challenging tasks due to the complex structure of the head end, feeding structures, and copulatory apparatus of these species. Due to their large size, the thick cuticle often makes it difficult to study leptosomatids using light microscopy. Therefore, the simultaneous use of several microscopy techniques (e.g., light, electron scanning, and laser confocal methods), image processing techniques, and molecular analysis can help overcome data limitations in studies of marine nematodes. Currently, there are only a few examples of the use of an integrative approach to study marine free-living nematodes, but the results obtained in these analyses reflected the high efficiency of this approach (for example, De Oliveira et al., 2012; Derycke et al., 2010a; Fonseca et al., 2008; Leduc and Zhao, 2016, 2019).

Examination of the material collected by the German-Russian and the Russian-German deep-sea expeditions in the North-Western Pacific revealed that species of the family Leptosomatidae regularly occur in macrobenthic samples. And some members of the family can be concluded as new to science.

The purpose of this work is to offer an integrative study of the new

* Corresponding author.
E-mail address: mordukhovich.vv@dvfu.ru (V.V. Mordukhovich).

https://doi.org/10.1016/j.pocean.2019.102160

Available online 09 August 2019

genus and two new species of Leptosomatidae with a discussion of the systematic position of the family within the order Enoplida.

2. Material and methods

2.1. Study area and sampling

Samples were collected in several locations during KuramBio I (July-August 2012), SokhoBio (July-August 2015) and KuramBio II (August-September 2016) expeditions to the Kuril–Kamchatka Trench and adjacent northwest Pacific at water depths of 3350–9290 m (Fig. 1, Table 1). Specimens collected by Agassiz trawl (AGT), epibenthic-sledge (EBS) and giant-boxcorer (GKG). On deck, the sediment from the AGT was sieved through a 1000-μm mesh size, and the upper layer of sediment (0–20 cm) from the GKG was carefully sieved through 1000-, 500- and 300-μm mesh sizes. Immediately after sieving, samples from AGT and GKG were sorted in seawater using stereomicroscopes, and nematodes were removed and fixed in 10% formalin for morphological studies and in DESS for DNA studies. On deck, the samples from EBS were immediately transferred into chilled (−20 °C) 96% ethanol and kept in a −20 °C freezer for at least 48 h for subsequent DNA studies. In the laboratories of the ship and in the home institutes, sorting of the fauna was done on ice in order to avoid DNA decomposition.

2.2. Morphological analysis

Nematodes were picked out from the formalin fixed samples under a stereoscopic microscope, transferred to glycerin using the Seinhorst's

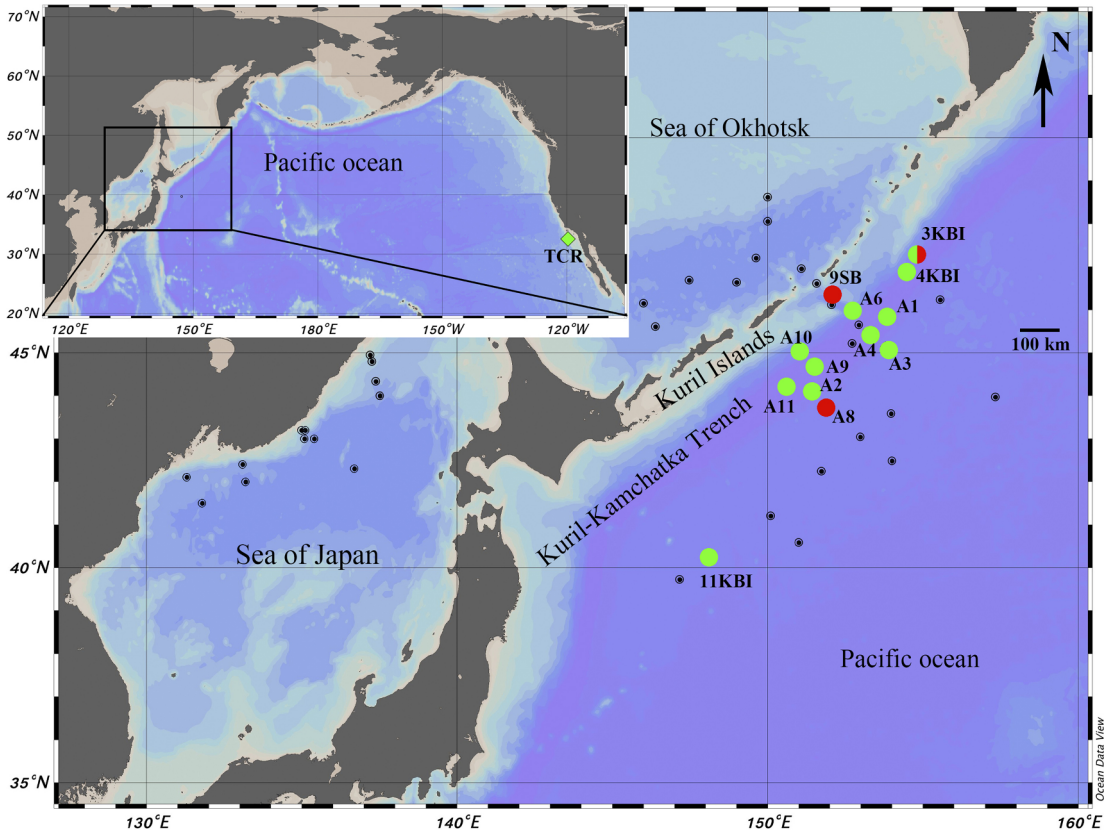

Fig. 1. Map of the investigated area. Dot means sampled station, red dot – presence of *Platonova magna* sp. nov., green dot – presence of *Platonova verecunda* sp. nov, green diamond – *Synonchus* sp. TCR_206. (For interpretation of the references to colour in this figure legend, the reader is referred to the web version of this article.)

Table 1
Localities, depth and sampling data.

Species	Cruise	Area	Longitude midpoint [degree north]	Latitude midpoint [degree east]	Average depth [m]	Date [year/month/day]
Platonova magna sp. nov.	KuramBio I	3	47.2	154.7	4991	2012/08/04-05
Platonova magna sp. nov.	SokhoBio	9	46.2	152.1	3374	2015/07/25-27
Platonova magna sp. nov.	KuramBio II	A8	43.8	151.8	5152	2016/08/18-20
Platonova verecunda sp. nov.	KuramBio I	3	47.2	154.7	4991	2012/08/04-05
Platonova verecunda sp. nov.	KuramBio I	4	47.0	154.5	5756	2012/08/06-07
Platonova verecunda sp. nov.	KuramBio I	11	40.2	148.1	5347	2012/08/29-30
Platonova verecunda sp. nov.	KuramBio II	A1	45.9	153.8	8208	2016/08/21-23
Platonova verecunda sp. nov.	KuramBio II	A2	44.1	151.4	6490	2016/09/18-19
Platonova verecunda sp. nov.	KuramBio II	A3	45.2	153.7	5743	2016/09/08-09
Platonova verecunda sp. nov.	KuramBio II	A4	45.5	153.2	8724	2016/09/06
Platonova verecunda sp. nov.	KuramBio II	A6	45.9	152.8	6114	2016/08/25-27
Platonova verecunda sp. nov.	KuramBio II	A9	44.7	151.5	8235	2016/09/12-17
Platonova verecunda sp. nov.	KuramBio II	A10	45.0	151.1	5477	2016/09/16
Platonova verecunda sp. nov.	KuramBio II	A11	44.2	150.6	9436	2016/09/20-21

(1959) rapid method as modified by De Grisse (1969), and mounted on permanent slides. Drawings and DIC (differential interference contrast) photographs were made on an optical microscope Olympus BX 53 with the aid of a drawing tube and a digital camera respectively.

Two individuals of each species fixed in formalin were cut to obtain a piece containing the anterior end. The specimens were then rinsed in the distilled water. After dehydratation in graded ethanol series and ethanol-acetone mixture, the specimens were embedded in Spurr resin (Spur, Sigma). Semithin transverse sections (0.5 μm) were cut with a Leica Ultracat E Ultratome. Obtained sections were stained with methylene blue and examined using light microscope Zeiss Axio Imager Z.2. The acquired images were then adjusted for contrast and brightness using the ImageJ image processing software.

Two formalin fixed males of each species were prepared to study the structure of spicules and head end by the laser scanning confocal microscopy (LSCM) using natural autofluorescence (Fadeeva and Zograf, 2010; Zullini and Villa, 2006). The head end and the cloacal part of the body were cut off, washed with distilled water and then the soft tissues were removed in 10% solution of sodium hypochlorite (NaOCl), then washed again with distilled water and glycerol slides were prepared. Microscopic examination was done using an Olympus BX 53 light microscope and a confocal microscope Leica LSM SPE. Fluorescence image stacks were registered in the 488 nm (green) channel. The scanning step size was usually 0.5 mm. The number of optical sections in a series ranged from 30 to 70, depending on the size of the specimen.

For the scanning electron microscopy, specimens were gradually dehydrated in a series of baths of increasing ethanol content, dried in a critical-point dryer, sputtercoated with gold and observed and imaged with a Ziess Evo 40 scanning electron microscope (SEM). Longitudinal sections were obtained by cutting the head end along the axis of symmetry.

Type specimens are preserved in the collection of the Zoological

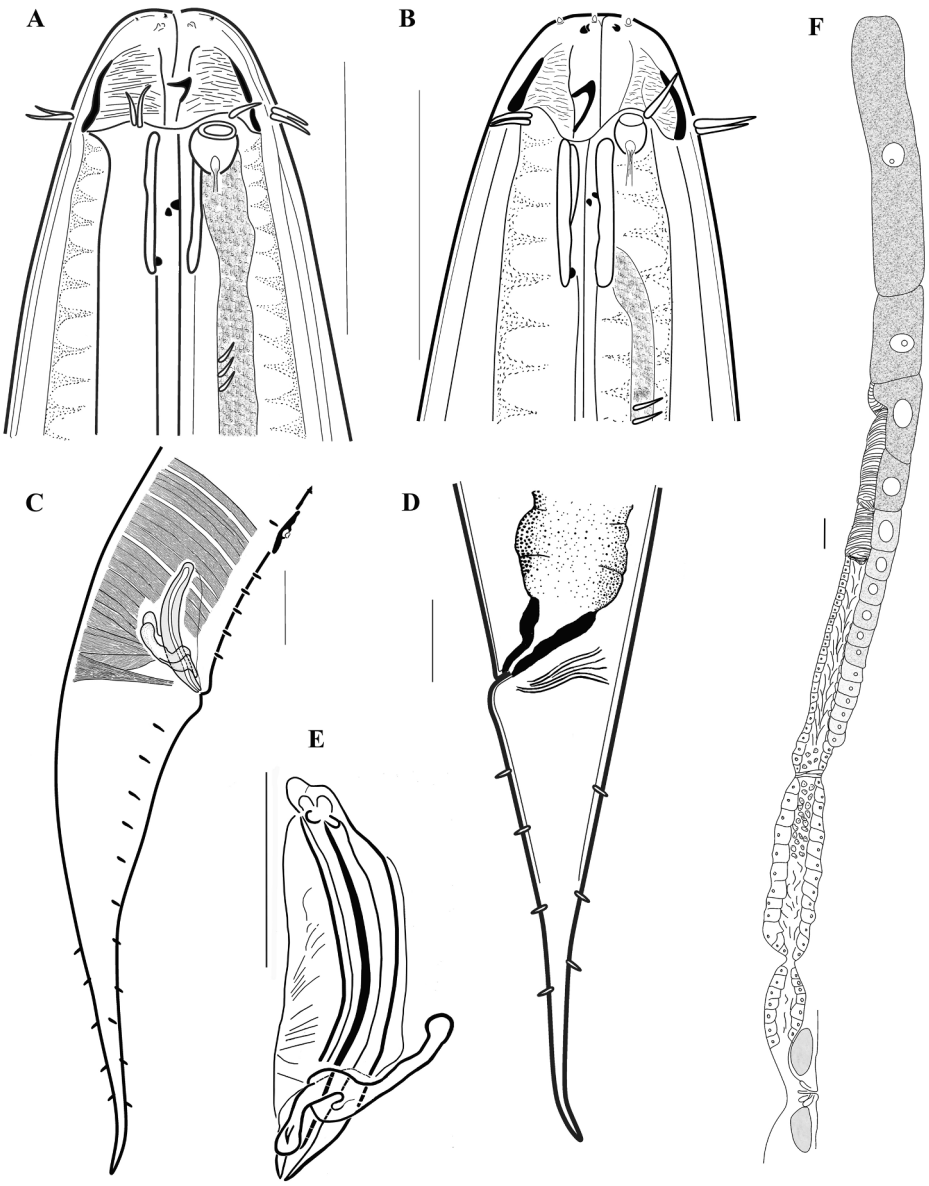

Fig. 2. *Platonova magna* sp. nov. (A) Female head. (B) Male head. (C) Male tail. (D) Female tail. (E) Spicules and gubernaculum, lateral view. (F) Female reproductive systems, anterior branch. Scale bars: 100 μm.

Museum of Far Eastern Federal University, Vladivostok, Russia.

Abbreviations of the measured variables in the description are: a – body length divided by maximum body diameter; b – body length divided by pharyngeal length; c' – tail length divided by corresponding body diameter at cloacal level; c – body length divided by tail length; c. b. d. – corresponding body diameter (μm); L – body length (μm); V – distance of the vulva from the anterior end (μm); V (%) – distance of the vulva from the anterior end as percentage of body length (%).

2.3. Molecular analyses

Nematodes were picked out from the DESS or ethanol fixed samples under a stereoscopic microscope, mounted on temporary slides with sterile distilled water and observed at different magnifications using a light microscope (Olympus BX 53) with differential interference contrast, and equipped with a digital camera. After the vouchering DNA from the whole body of adult nematodes was extracted using a hotshot extraction method (Truett et al., 2000) in compliance with described protocol. PCR mixture contained 5 μl Go Taq Green Master Mix (Promega corp, Madison, WI, USA), 0.5 μM of each primer, 3 μl of nuclease-free water (Ambion) and 1 μl of genomic DNA. Fragments of the nuclear ribosomal DNA and internal transcribed spacers (18S rDNA, ITS1, 5.8S rDNA, ITS2 and D2-D3 region of 28S rDNA) and the mitochondrial cytochrome oxidase c subunit 1 (COI) genes were amplified. For 18S rDNA, we used the primer set SSU_F_03 and SSU_R_81 (Blaxter et al., 1998) which amplifies a fragment of ca 1800 bp. The internal transcribed spacer (ITS) region was amplified with the primers Vrain2F and Vrain2R (Vrain et al., 1992) which amplifies a fragment of ca 1200 bp. whereas the D2-D3 region of the 28S ribosomal DNA region was amplified using the primers D2a and D3b (Nunn, 1992). The length of the obtained amplicon was 700 bp. For COI, we used the primer set JB3 (Bowles et al., 1992) and JB5 (Derycke et al., 2005) which amplifies a fragment of *ca* 400 bp. PCR products were visualized on a 1.5% TBE agarose gel GelDoc XR + imaging systems (BioRad). Each PCR fragment was purified using Exonuclease I (ExoI) and Thermosensitive Alkaline Phosphatase (FastAP) (Thermo Fisher Scientific Inc., USA). PCR products were cycle sequenced using BigDye Terminator v.3.1 Cycle Sequencing Kit (Applied Biosystems, Inc.), and bidirectionally sequenced on an ABI 3130XL automated sequencer. We use additional primers to sequence 18S rDNA amplicons: SSU_F_24_1 (Meldal et al., 2007) and SSU_R_13 (Blaxter et al., 1998). MEGA7 (Kumar et al., 2016) and FinchTV were used to edit and assemble double stranded sequences. Also, MEGA7 was used for calculated inter- and intraspecific COI and ITS (in this article abbreviation for genetic marker contained ITS1 − 5.8S rDNA – ITS2) K2P distances. ABGD analysis (www.abi.snv.jussieu.fr/public/abgd/abgdweb.html, Puillandre et al., 2012) was used for species delimitation and establish taxonomic status of sequenced specimens, using relative gap width (X = 1.0) and intraspecific divergence (P) values between 0.005 and 0.100 with the K2P model.

The obtained sequences were aligned using M-Coffee (Wallace et al., 2006) integrated into the T-Coffee software. PartitionFinder 2.1.1 (Lanfear et al., 2012) was used to select the best-fit partitioning scheme and models separately for each codon position of COI as well as ribosomal loci using the greedy algorithm with linked branch lengths for the corrected Bayesian Information Criterion. The best models of nucleotide substitution for ribosomal loci was GTR (Tavare, 1986) plus I (a proportion of invariable sites) whereas for 1 and 3 COI codon positions the best models were HKY + G (Hasegawa et al., 1985) and F81 + G (Felsenstein, 1981) for 2 position. Sequences of *Platonova magna* sp. nov. and *P. verecunda* sp. nov. obtained in this study have been deposited in GenBank (accession numbers MK007141-MK007146 for COI, MK007570-MK007575 for 18S rDNA, MK007576-MK007581 for ITS1 – 5.8S rDNA – ITS2 and MK007564-MK007569 for 28S rDNA).

Fig. 3. *Platonova magna* sp. nov. Light microscopy (A) Female body. (B) Male body. Scale bars: 1000 μm.

SSU rDNA and *LSU* rDNA sequences were used for analyses of the position of the family Leptosomatidae in order Enoplida and *LSU* rDNA and COI sequences were used to resolve phylogenetic relationships within leptosomatids. Each tree was made by Bayesian Inference and Maximum likelihood, however, we show only a Bayesian tree with the addition bootstrap supports in the branch nodes of ML tree with the same topology. In addition to our sequences, we used GenBank data and only sequences longer than 1550 bp and 590 bp were included in the final SSU and LSU phylogenetic analyses respectively. For COI phylogeny we used I3-M11 region longer than 320 bp. Bayesian phylogenetic analyses were conducted with MrBayes v. 3.2.7 (Ronquist and Huelsenbeck, 2003). Bayesian Inference was performed with two independent runs of Metropolis-coupled Markov chain Monte Carlo analyses, with each run comprising one cold chain and three heated chains at a heating temperature of 0.06 for 18S tree and default temperature of 0.1 for 28S tree. The chains were run for 5 million generations and sampled every 500 generations. A burn-in of 500,000 generations (or 10% of the sampled trees) was used. Moreover, trace files were visually inspected in Tracer 1.7 (Rambaut et al., 2018). RAxML v. 8.2.4 (Stamatakis, 2006) was used to conduct a maximum likelihood (ML) and bootstrap analysis (1000 replications) using the GTR plus G model. FigTree v. 1.4.4 was used to visualize phylogenetic trees after analysis.

3. Results

3.1. Morphological analysis

Family Leptosomatidae Filipjev, 1916
Subfamily Synonchinae Platonova, 1970
Diagnosis (from Platonova, 1976).

Cephalic capsule short, rather thin-walled, but distinctly developed. Cephalic suture may be straight, but often bends and forms lobes and grooves. Interlobular grooves wide and not divided into furrows; formed by smoother curve of cephalic suture. All grooves identical in shape; lateral ones, in which amphids are located, do not differ in any way from the rest. Amphids may be situated inside lateral grooves as well as below level of cephalic suture. Cephalic ring narrow. Oral cavity small, often armed with onchia. Nerve ring encircles pharynx most often in its anterior third. Tail in majority of genera stretched but claviform at end. Posterior end in males covered with a large number of setae. Preneural part of body in both male and female usually covered with numerous long setae. Photosensitive eyes absent.

List of valid genera (Bezerra et al., 2019)
Anivanema Platonova, 1976
Corythostoma Hope and Murphy, 1972
Eusynonchus Platonova, 1970
Macronchus Inglis, 1964
Paratuerkiana Platonova, 1970
Sadkonavis Platonova, 1979
Synonchoides Wieser, 1956
Synonchus Cobb, 1894

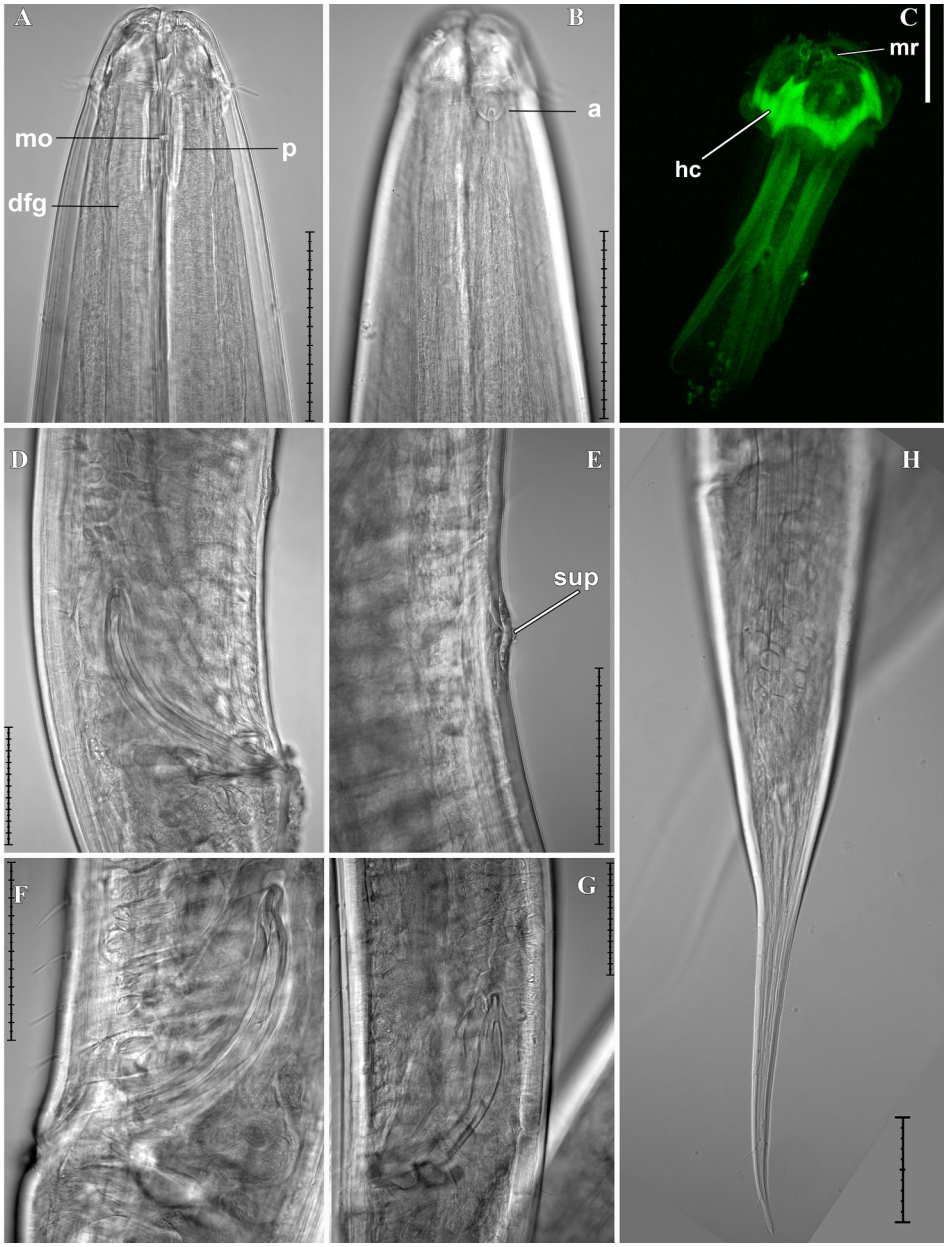

Fig. 4. *Platonova magna* sp. nov. A-B, D-H light microscopy, DIC. C confocal microscopy. (A) Anterior end of male. (B) Anterior end of male. (C) Head capsule of male. (D) Male copulative apparatus. (E) Supplementary organ. (F) Male copulatory apparatus. (G) Male copulatory apparatus. (H) Male tail. Scale bars: 100 µm. Abbreviations: a - amphid; mr - mandibular ridge; dfg - dorsal pharyngeal gland; hc - head capsule; mo - microonchium; p - cuticular beams; sup - supplementatry organ.

Triaulolaimus Platonova, 1979
Tuerkiana Platonova, 1970
Genus *Platonova* **gen. nov.**

Genus description. Synonchinae. Very large nematodes. Cephalic capsule relatively long, interlobular grooves wide. Three well-developed lips. Amphideal fovea big, pocket-shaped, located in lateral grooves. Six small inner labial papillae (2 on each lip); six outer labial setae and four cephalic setae in one circle, relatively equal in length. Short post-amphideal setae present. Cheilostome with three mandibular ridge, odontia present. Single dorsal onchium in the anterior part of pharyngostome. The posterior part of pharyngostome is reinforced with 6 cuticular beams (each 2 on the dorsal and two ventrosublateral sectors) and contains microonchia. Female amphidelphic, gonads antidromic. Male diorchic, testes opposed and outstretched. Spicules curved, gubernaculum with dorsal and ventral processes. Pre-cloacal ventromedian supplement and subventral pre-cloacal sensilla present. Tail conical anteriorly, filiform posteriorly.

Etymology. The genus name is given in honour of Tatyana Alekseevna Platonova, a russian nematologist who intensively studied the family Leptosomatidae

Differential diagnosis. The new genus differs from other known Synonchinae genera by the following characters: tail shape (conical anteriorly and filiform posteriorly), pronounced division of pharyngostome into 2 parts, one dorsal tooth in the anterior part of pharyngostome, 6 cuticular beams and microonchia in the posterior part of pharyngostome. Moreover, the structure and armature of the stoma sharply distinguish the new genus from all other genera of the family Leptosomatidae.

Richard Warwick (1973) has described *Synonchus alisonae* (from the Indian ocean) with a very similar to *Platonova* **gen. nov.** set of characters according to the presented drawings (tail with filiform part, presence of cuticular beams and microonchium in pharyngostome), however, did not provide their explanation in the text. We state that this species belongs to genus *Platonova* **gen. nov.**

Remark. *Platonova* **gen. nov.** resembles *Metacylicolaimus* (Cylicolaiminae) in the tail shape, funnel-shaped buccal cavity, well-developed dorsal tooth, presence of pre-cloacal ventromedian supplement, absence of photosensitive eyes. However, in addition to the already mentioned differences in the structure and armature of pharyngostome, in *Metacylicolaimus* species cephalic capsule is less developed and armature absent in cheilostome.

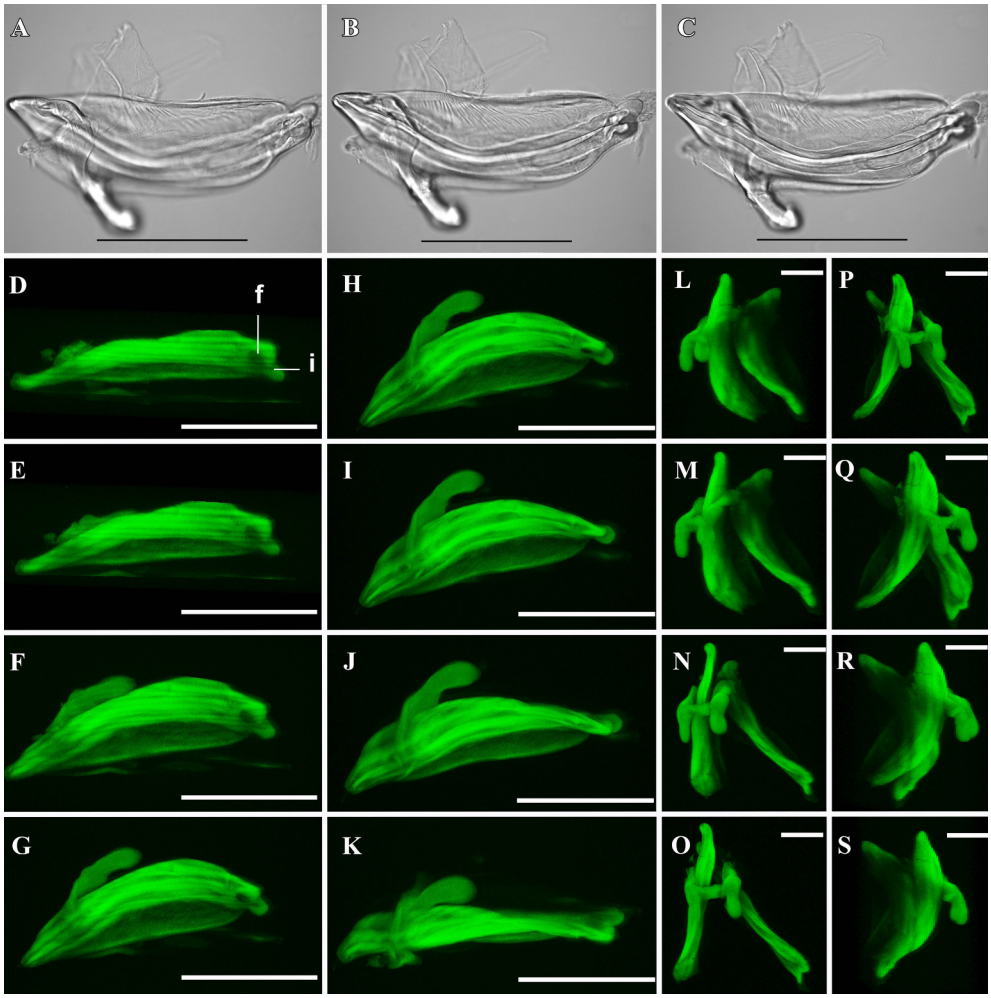

Fig. 5. *Platanova magna* sp.nov. Extracted copulatory apparatus of male. (A-C) Light microscopy, DIC. (D-S) Confocal microscopy. (A-C) Copulatory apparatus at different focal planes, lateral view. (D-K) Copulatory apparatus at different angles of view (from ventral (D) to dorsal (K)). (L-S) Copulatory apparatus at different angels of view (from subventral (L) to dorsal (N-Q) and subdorsal (S)). Scale bars: A-K – 100 μm; L-S – 50 μm. Abbreviations: i - incision; f - fenestra.

Type species. *Platonova magna* **gen. et sp. nov.**

***Platonova magna* gen. et sp. nov.**

(Figs. 2–10, Table 2)

Measurements. See Table 2.

Type material. Three males (holotype and two paratypes) and three females (paratypes). The type species are deposited in the Zoological Museum of Far Eastern Federal University, Vladivostok, Russia (MN SB 9-9 Pm1). Paratypes are deposited in the Zoological Museum of Far Eastern Federal University, Vladivostok, Russia (MN SB 9-9 Pm1 and MN SB 9-9 Pm2).

Etymology. The species name is derived from the Latin magna (= great) and refers to the well-developed armature of buccal cavity of this species.

Description. *Males*.

Body large, cylindrical, tapering from about the level of the cardia towards the head (Fig. 3B). Cuticle thick, marked with fine transverse striations. Head blunt, rounded, bounded by three rounded lips each bearing a pair of small conical labial papillae (Figs. 2A, 4A, 10A, D). Six outer labial setae and four cephalic setae in one circle, equal in length, 15–20% *cbd* long, with nerve process often visible. There are two or three short setae about 60 μm posterior to amphid and a few other short setae scattered posteriorly to about the level of the nerve-ring. Cephalic capsule without prominent anterior lobes or tropis; six posterior lobes present. Interlobar incisions wide, simple, without posteriorly-directed arms; posterior lobe margin smooth (Figs. 2A, 4B, C). Amphids pocket-shaped with relatively small aperture, 7–9 μm wide by 3–5 μm high (Figs. 2A, 4B, 10D).

Cheilostome with three complexes of fused mandibular ridges and 2 odontia, ventrosublateral ones are about 5–6 μm wide and dorsal one is about 2–3 μm (Figs. 8a, 10B, G, I). The pharyngostome varies in appearance depending on the angle from which it is viewed. It is basically conical, anterior part contains a large solid dorsal tooth, ventrosublateral teeth absent. The posterior part of pharyngostome with 6 cuticular beams (each 2 on the dorsal and two ventrosublateral sectors), 43–51 μm long. There are two ventrosublateral microonchia at about the level of the middle of the cuticular beams and dorsal microonchium at the base of cuticular beams (Figs. 2A, 4A, 8j, k, 10H).

Dorsal pharyngeal gland lies in the center of the dorsal sector and opens into the posteriormost part of the buccal cavity (Figs. 4A, 8l). Subventral glands lie in the center of respective sector between the radial muscles (Fig. 8i, g). Near the base of anterior part of the pharyngostome subventral gland cells become continuous with a cuticularly lined ducts which proceed anteriorly in the cheilostome, the locations of the external orifices are uncertain (Fig. 8b–f). Subdorsal pharyngeal glands are sometimes well seen but in the anterior part of the pharynx each gland becomes very thin, imperceptible and not observed in serial cross sections of the head end. Pharynx largely muscular, undivided, cylindrical, slightly tapered anteriorly. Renette absent.

Lateral hypodermal chords with numerous large epidermal glands and loxometanemes of type I with caudal filaments (Fig. 9A–G). The ends of caudal filaments are often difficult to detect and exact number and length of metanemes cannot be determined.

Male reproductive system diorchic with opposed testes in left position to the intestine. Anterior gonad 6351 μm, posterior one 2055 μm.

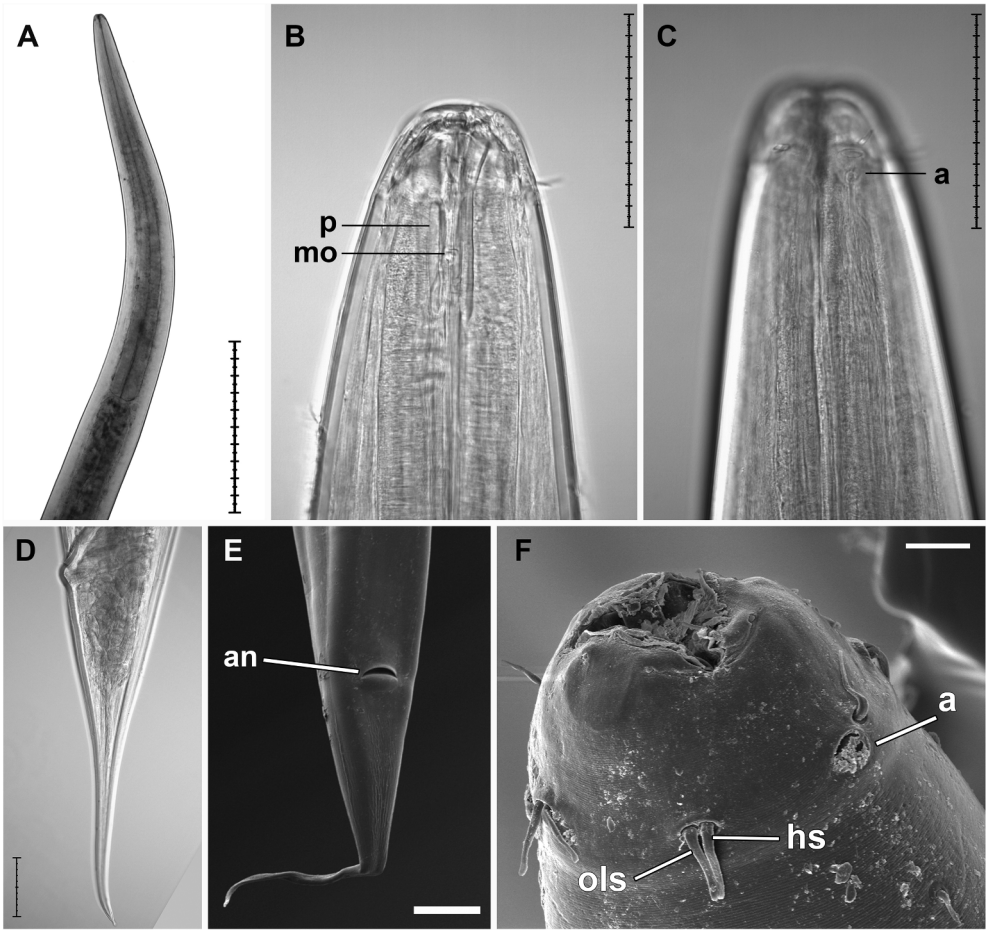

Fig. 6. *Platanova magna* sp.nov. (A-D) Light microscopy, DIC. (E-F) Scanning electron microscopy (A) Anterior end of female. (B) Female head end. (C) Female head end. (D) Female tail. (E) Female tail. (F) Female head end. Scale bars: A – 1000 μm; B-E - 100 μm; F - 10 μm. Abbreviations: a - amphid; an - anal opening; hs - head setae; mo - microonchium; ols - outer labial setae; p - cuticular beams.

Vas deferens heavily muscled (Fig. 9H), 8156 μm. Pre-cloacal ventromedian supplement present, 1.1–1.2 *abd* anterior to cloaca (Figs. 2C, 4D, E, 10C, F, J). Two rows of subventral peri-cloacal setae present (Figs. 4F, 10C, F). There are 6–9 setae in each row between cloaca and supplement, 18–23 anterior to supplement and 6–8 posterior to cloaca.

Spicules paired, fusiform, 1.3 *abd* long. Capitulum well developed, wide, with incision and circular fenestra. Spicules are usually somewhat twisted (Fig. 5D–K, L–S), and the structure of the capitulum is often not obvious in light microscope (Fig. 4D, F, G). Calomus indistinct. Lamina with wide vellum. Gubernaculum composed of two symmetrical wings, joined together by one centered ventral piece, crura with membrane embracing the spicule and with ventral expansion of an intricate shape.

Tail conical anteriorly, filiform posteriorly, with scattered short setae (Fig. 2C, 4H, 10K). Caudal glands absent.

Females. Similar to males, but with one short setae about 25 μm posterior to amphid (few other short setae scattered posteriorly to about the level of the nerve-ring) and slightly shorter on tails. Reproductive system amphidelphic with two opposed and reflexed ovaries (Fig. 2F, 7A, B); in two females both branches to the left of intestine and in one female to the right of intestine. Vulva situated at ~ 1/2 of body length. Anterior ovary 1656–2934 μm, posterior one 2284–2450 μm, anterior uterus 983–1249 and posterior one 970–1200 μm; mature eggs 210–241 μm wide by 746–1151 μm long. The oviduct differentiated into a narrow part with collapsed lumen and

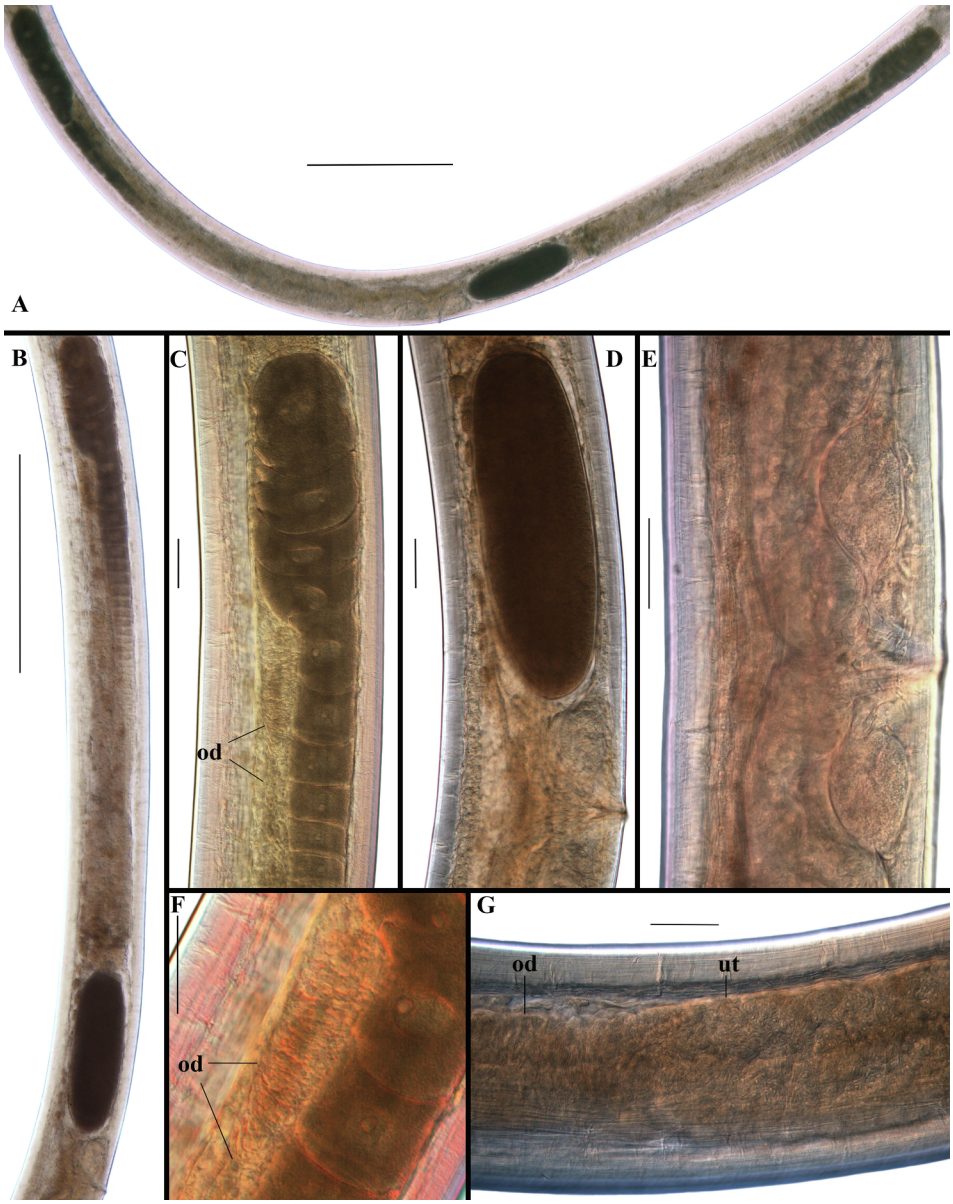

Fig. 7. *Platonova magna* sp. nov. Light microscopy, DIC. (A) Female reproductive system. (B) Female reproductive system, anterior branch. (C) Ovary and oviduct. (D) Vulvar region and uterus with egg. (E) Vulvar region. (F) Narrow part of the oviduct. (G) Wider part of the oviduct and uterus. Scale bars: A, B - 1000 μm; C-G -100 μm. Abbreviations: ov - oviduct; ut - uterus.

wider part (close to the uterus) (Fig. 7C, F, G). Spermathecae absent, the sperm cells scattered along the uterus and expanded part of oviduct.

Locality. Eastern slope of the Kuril Islands and abyssal of the North-eastern Pacific, water depth 3374–5152 m (Fig. 1, Table 1).

Diagnosis and relationships. *Platonova magna* sp. nov. is characterised by the combination of following characters: very large body size, cheilostome with three complexes of fused mandibular ridges and 2 odontia (ventrosublateral ones about 5–6 μm wide and dorsal one about 2–3 μm), posterior part of pharyngostome with 6 cuticular beams 43–51 μm long, two ventrosublateral microonchia at about the level of the middle of the cuticular beams and dorsal microonchium at the base of cuticular beams, one ventral pre-cloacal supplement situated 190–210 μm anterior to cloaca, spicules 214–243 μm, with wide vellum, capitulum with incision ending in circular fenestra.

Platonova magna sp. nov. can be differentiated from *P. alisonae* by the larger body size (18333–23615 μm *vs* 10030–11700 μm), by the number of supplements (1 *vs* 2), by the presence of vellum. *Platonova magna* sp. nov. differs from *P. verecunda* sp. nov. in the length of cuticular beams in pharyngostome (43–54 μm *vs* 19–27 μm), in the position of ventrosublateral microonchia (middle *vs* anterior part of the cuticular beams), and in the length of spicules (214–243 μm *vs* 152–161 μm).

Nucleotide sequences. GenBank accession numbers MK007141 -

Fig. 8. *Platonova magna* sp.nov. Anterior end of the male showing levels of sectioning (scale bar - 100 μm). Light microphotographs of transverse sections. Dorsal to the left. (a) Mouth opening at the level of mandibular ridges. (b) Buccal cavity at the level of ventrosublateral pharyngeal gland ducts. (c) Buccal cavity at the level of head capsule. (d) Buccal cavity at the level of dorsal onchium. (e) Buccal cavity at the level of amphids and head setae. f. Buccal cavity at the level of amphids. (g) Buccal cavity at the level of ventrosublateral pharyngeal glands and cuticular beams. (h) Buccal cavity at the level of ventrosublateral microonchium and cuticular beams. (i) Buccal cavity at the level of ventrosublateral microonchia and cuticular beams. (j) Buccal cavity at the level of dorsal microonchium and cuticular beams. (k) Posterior part of the buccal cavity at the level of dorsal microonchium and cuticular beams. (l) Posteriormost part of the buccal cavity. Scale bars: 10 μm. Abbreviations: a - amphid; dmr - dorsal mandibular ridge; ds - dorsal side; fg - pharyngeal gland; fgd - pharyngeal gland duct; hc - head capsule; mo - microonchium; o - dorsal onchium; odfg - orifice of the dorsal pharyngeal gland; p - cuticular beams; vlmr - ventrosublateral mandibular ridge.

MK007143 (COI), MK007570 - MK007572 (18S rDNA), MK007576 - MK007579 (ITS1 – 5.8S rDNA – ITS2) and MK007564- MK007566 (28S rDNA).

***Platonova verecunda* sp. nov.**

Measurements. See Table 2.

Type material. Three males (holotype and two paratypes) and three females (paratypes). The type species are deposited in the Zoological Museum of Far Eastern Federal University, Vladivostok, Russia (MN KBII 98 Pv1). Paratypes are deposited in the Zoological Museum of Far Eastern Federal University, Vladivostok, Russia (MN KBII 98 Pv1 and KBII 103 Pv1).

Etymology. The species name is derived from the Latin *verecunda* (=modest) and refers to the moderately developed armature of buccal cavity of this species.

Description. *Males*.

Body large, cylindrical, tapering from about the level of the cardia towards the head (Fig. 12A). Cuticle thick, marked with fine transverse striations. Head blunt, rounded, bounded by three rounded lips each bearing a pair of small conical inner labial papillae (Figs. 11B, 17C, D). Six outer labial setae and four cephalic setae in one circle, equal in length, 17–26% *cbd* long, with nerve process often visible. There are 2–4 short setae about 40–60 μm posterior to amphid and a few other

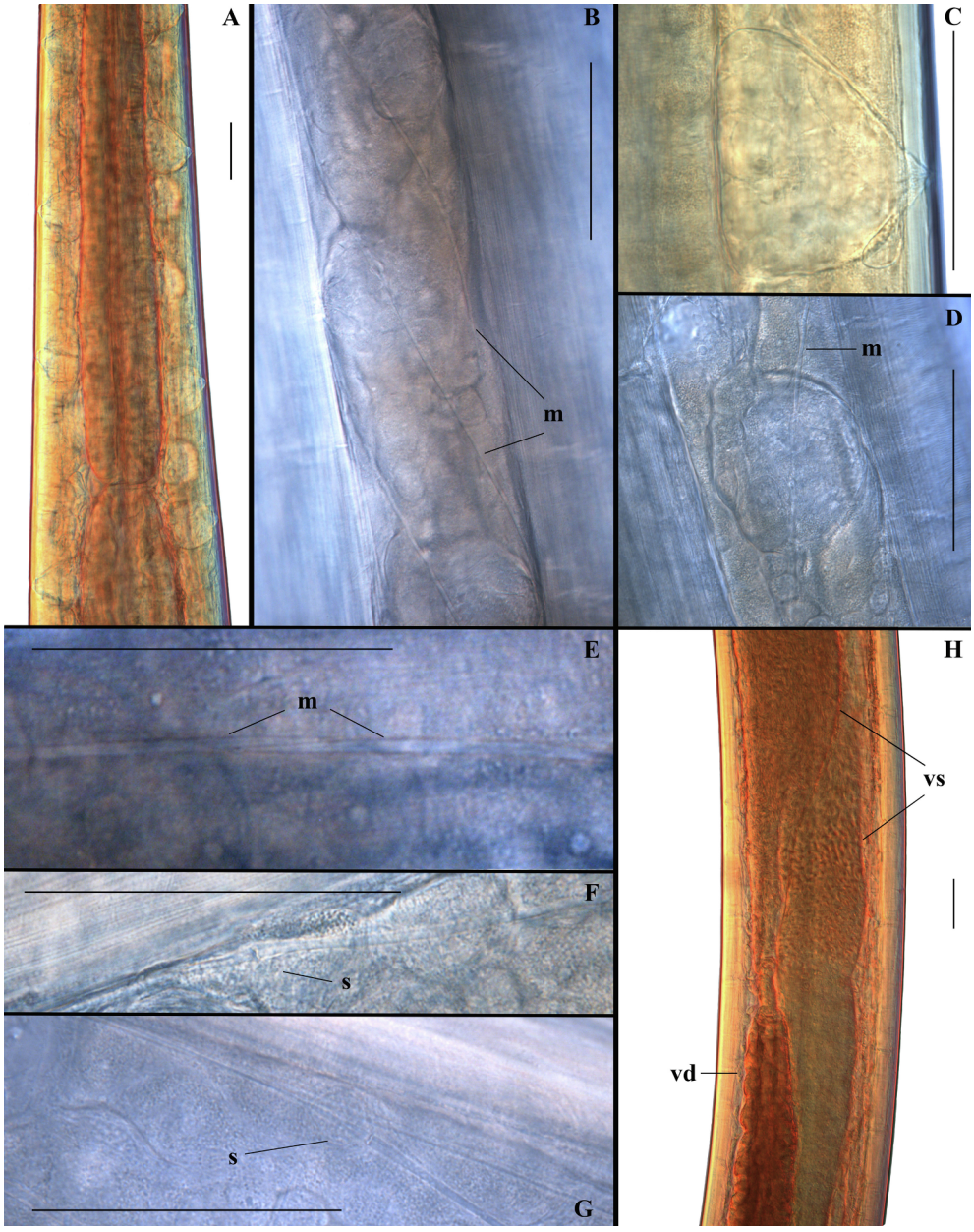

Fig. 9. *Platonova magna* sp. nov. Light microscopy, DIC. (A) Pharyngeal region with large epidermal glands, ventral view. (B) Lateral hypodermal chord with large glands and metanemes, lateral view. (C) Epidermal gland, ventral view. (D) Epidermal gland and metaneme, lateral view. (E-G) Metanemes. (H) Male reproductive system (*vas deferens* and *vesicula seminalis*), lateral view. Scale bars: 100 μm. Abbreviations: m - metaneme; s - scapulus, vd - *vas deferens*; *vs* - *vesicula seminalis*.

short setae scattered posteriorly to about the level of the nerve-ring (Fig. 17A, B). Cephalic capsule without prominent anterior lobes or tropis; six posterior lobes present. Interlobar incisions wide, simple, without posteriorly-directed arms; posterior lobe margin smooth (Fig. 11B). Amphids pocket-shaped with relatively small aperture, 7–9 μm wide by 3–5 μm high (Fig. 17B, D, J, K).

Cheilostome with three mandibular ridges (Fig. 16a). The pharyngostome conical, anterior part contains a large solid dorsal tooth, ventrosublateral teeth absent. The posterior part of pharyngostome with 6 weakly developed cuticular beams (each 2 on the dorsal and two ventrosublateral sectors), 19–27 μm long. There are two ventrosublateral microonchia at the level of apical part of the cuticular beams and dorsal microonchium at the base of cuticular beams (Figs. 14A, 16e–g, 17H, I).

Dorsal pharyngeal gland lies in the center of the dorsal sector and opens into the posterior part of the buccal cavity (Fig. 16h). Subventral glands lie in the center of respective sector between the radial muscles (Fig. 16e–h). Near the base of anterior part of the pharyngostome subventral gland cells become continuous with a cuticularly lined ducts which proceed anteriorly in the cheilostome, the locations of the external orifices are uncertain (Fig. 16b–d). Subdorsal pharyngeal glands sometimes are well seen but in the anterior part of the pharynx each gland becomes very thin, imperceptible and not observed in serial cross sections of the head end. Pharynx largely muscular, undivided, cylindrical, slightly tapered anteriorly. Renette absent.

Lateral hypodermal chords with numerous loxometanemes of type I with caudal filaments (Fig. 14D–E). The ends of caudal filaments are often difficult to detect and exact number and length of metanemes

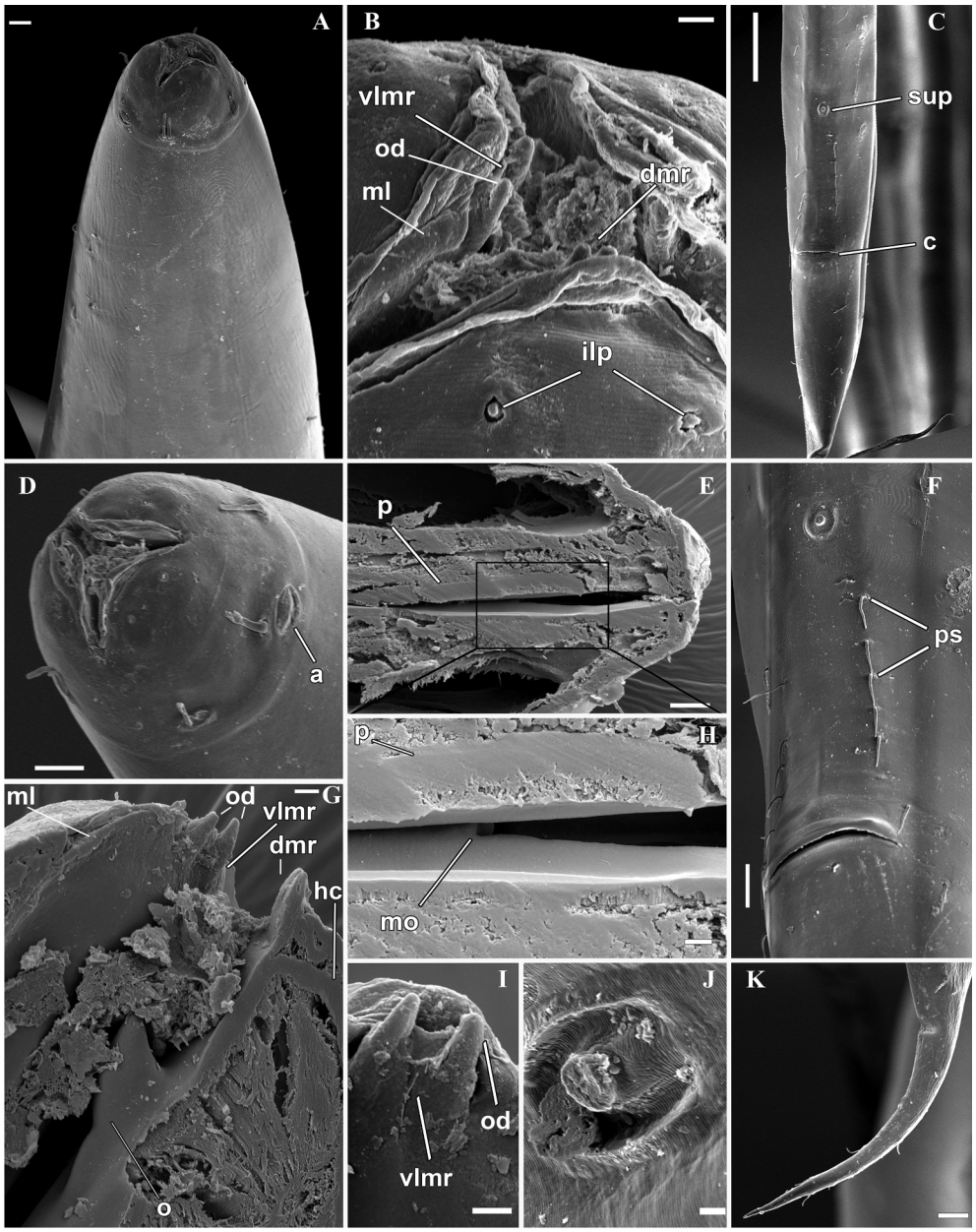

Fig. 10. *Platonova magna* sp. nov. Scanning electron microscopy. (A) Male anterior end. Subventral view. (B) Mouth opening with mandibles. (C) Posterior end of the male, ventral view. (D) Male head, anterior view. (E) Longitudinal section through the buccal cavity with cuticular plates. (G) Longitudinal section through the anterior part of buccal cavity with dorsal onchium. (H) Posterior part of buccal cavity with ventrosublateral microonchium. (F) Precloacal region of the male, ventral view. (I) Mandibular ridge. (J) Supplementary organ. (K) Male tail tip. Scale bars: A, D; E – 10 μm; B, G, H, I, J – 2 μm; F, K – 20 μm; C – 100 μm. Abbreviations: a - amphid; c - cloacal opening; dmr - dorsal mandibular ridge; hc - head capsul; hs - head setae; ilp - inner labial papillae; mg - mandibular ridge; mo - microonchium; o - dorsal onchium; od - odontium; ols - outer labial setae; p - cuticular beams; ps - precloacal setae; sup - supplementary organ; vlmr - ventrosublateral mandibular ridge.

Table 2
Morphometrics (μm) of *Platonova magna* sp. nov. and *Platonova verecunda* sp. nov.

	Platonova magna sp. nov.						*Platonova verecunda* sp. nov.					
	HT♂	♂	♂	♀	♀	♀	HT♂	♂	♂	♀	♀	♀
Amphid from anterior end	38	27	38	26	37	30	28	31	32	30	27	27
Anal body diam.	183	187	163	151	175	170	123	171	158	150	133	121
Beam length	53	45	43	47	51	54	25	25	27	27	19	25
Head diam. at level of cephalic setae	74	65	70	75	76	73	56	64	65	65	57	59
L	20,399	19,903	18,333	19,890	21,250	23,615	18,029	21,518	20,159	21,902	15,857	17,670
Length of cephalic setae	14	12	13	11	13	12	13	12	16	17	14	10
Maximum body diam.	430	383	335	305	397	395	278	325	305	300	235	245
Nerve ring from anterior end	750	753	765	790	833	803	661	775	765	667	645	569
Pharyngeal length	2350	2239	2298	2298	2537	2486	2046	2176	2026	2060	2025	1981
Spicule length	239	243	214	–	–	–	152	161	160	–	–	–
Supplement from cloaca	210	210	190	–	–	–	170	294	233	–	–	–
Tail length	704	665	735	671	679	617	778	767	697	661	663	758
V	–	–	–	9358	10,845	11,906	–	–	–	10,948	7988	8494
V (%)	–	–	–	47.0	51.0	50.4	–	–	–	50,0	50,4	48.1
a	47.4	52.0	54.7	65.2	53.5	59.8	64.9	66.2	66.1	73.0	67.5	72.1
b	8.7	8.9	8.0	8.7	8.4	9.5	8.8	9.9	10.0	10.6	7.8	8.9
c	29.0	29.9	24.9	29.6	31.3	38.3	23.2	28.1	28.9	33.1	23.9	23.3
c'	3.8	3.6	4.5	4.4	3.9	3.6	6.3	4.5	4.4	4.4	5.0	6.3

cannot be determined.

Male reproductive system diorchic with opposed testes in left position to the intestine. Anterior gonad 5316–5739 μm, posterior one 989–3674 μm. *Vas deferens* heavily muscled, 7204–10636 μm. Precloacal ventromedian supplement present, 1.4–1.7 *abd* anteriorly to cloaca (Figs. 13D, 17E, F). Two rows of subventral peri-cloacal setae present (Fig. 17E, G). There are 6–7 setae in each row between cloaca and supplement, 7–8 anterior to supplement and 4–5 posterior to cloaca.

Spicules paired, fusiform, 0.9–1.2 *abd* long. Capitulum well developed, wide, with circular fenestra (Fig. 13H, J). Because of the small torsion of spicules, the structure of the capitulum is often not obvious. Calomus indistinct. Lamina with a well pronounced "crack" on the dorsal side, wide vellum present (Fig. 13G, H). Gubernaculum composed of two symmetrical wings, joined together by one centered ventral piece, and the crura with membrane embracing the spicule and ventral expansion of an intricate shape.

Tail conical anteriorly, filiform posteriorly, with scattered short setae.

Females. Similar to males. Reproductive system amphidelphic with two opposed and reflexed ovaries (Figs. 11F, 15A, B); in two females both branches to the left of intestine and in one female anterior ovary to the right of intestine while location of posterior ovary is unclear. Vulva situated at ~1/2 of body length. Anterior ovary 1667–2564 μm, posterior one 1650–2428 μm, anterior uterus 596–908 and posterior one 906–917 μm; mature eggs 152–165 μm wide and 702–708 μm long. The oviduct differentiated into a narrow part with collapsed lumen and wider part (close to the uterus) (Fig. 15C, F). Spermathecae absent, the sperm cells scattered along the uterus and expanded part of oviduct (Fig. 15F, G).

Locality. Kurile-Kamchatka Trench, water depth 4991–9436 m (Fig. 1, Table 1); off coast California, 32° 47′ 52.32″ N 120° 22′ 18.36″ W, water depth 2695 m (Bik et al., 2010a, 2010b).

Diagnosis and relationships. *Platonova verecunda* sp.nov. is characterised by the combination of following characters: very large body size, cheilostome with three mandibular ridges, posterior part of pharyngostome with 6 cuticular beams 19–27 μm long, two ventrosublateral microonchia at the level of apical part of the cuticular beams and dorsal microonchium at the base of cuticular beams, one ventral pre-cloacal supplement situated 170–294 μm anterior to cloaca, spicules 152–161 μm, with wide vellum, capitulum with circular fenestra.

Platonova verecunda n. sp. can be differentiated from *P. alisonae* by the larger body size (15857–21902 μm *vs* 10030–11700 μm), by the number of supplements (1 *vs* 2), and by the presence of vellum. *Platonova verecunda* n. sp. differs from *P. magna* n. sp. in the shorter cuticular beams in pharyngostome (19–27 μm *vs* 43–54 μm), in the position of ventrosublateral microonchia (anterior *vs* middle part of the cuticular beams), and in the shorter spicules (152–161 μm *vs* 214–243 μm).

Nucleotide sequences. GenBank accession numbers MK007144 - MK007146 (COI), MK007573 - MK007575 (18S rDNA), MK007581 - MK007583 (ITS1 – 5.8S rDNA – ITS2) and MK007567- MK007569 (28S rDNA).

3.2. Molecular analysis

3.2.1. DNA barcoding

A total of 3 specimens of each species were sequenced. The final alignment of the COI barcode region yielded 393 base pairs. The total pairwise K2P distance within *P. magna* sp. nov. ranged from 0.015 to 0.023, which is based on ten nucleotide substitutions. Three individuals of *P. verecunda* sp. nov. differed for two nucleotide substitutions (K2P distances 0.003–0.005). Most substitutions within species were observed only in the third position of the codons. Each sequenced specimen had a unique haplotype for the COI gene.

The average interspecific K2P distance (COI) between *P. magna* sp. nov. and *P. verecunda* sp. nov. was 0.128. Four nonsynonymous substitutions at positions 10, 86, 88, and 95 were observed between these species. The high differences between the two new species were also confirmed by ABGD analysis, which yielded 2 operational taxonomic units (OTU) using a 0.019–0.072 intraspecific divergence. We combined the COI sequences of two new species to compute the intergeneric distances within the family Leptosomatidae. A comparison of the

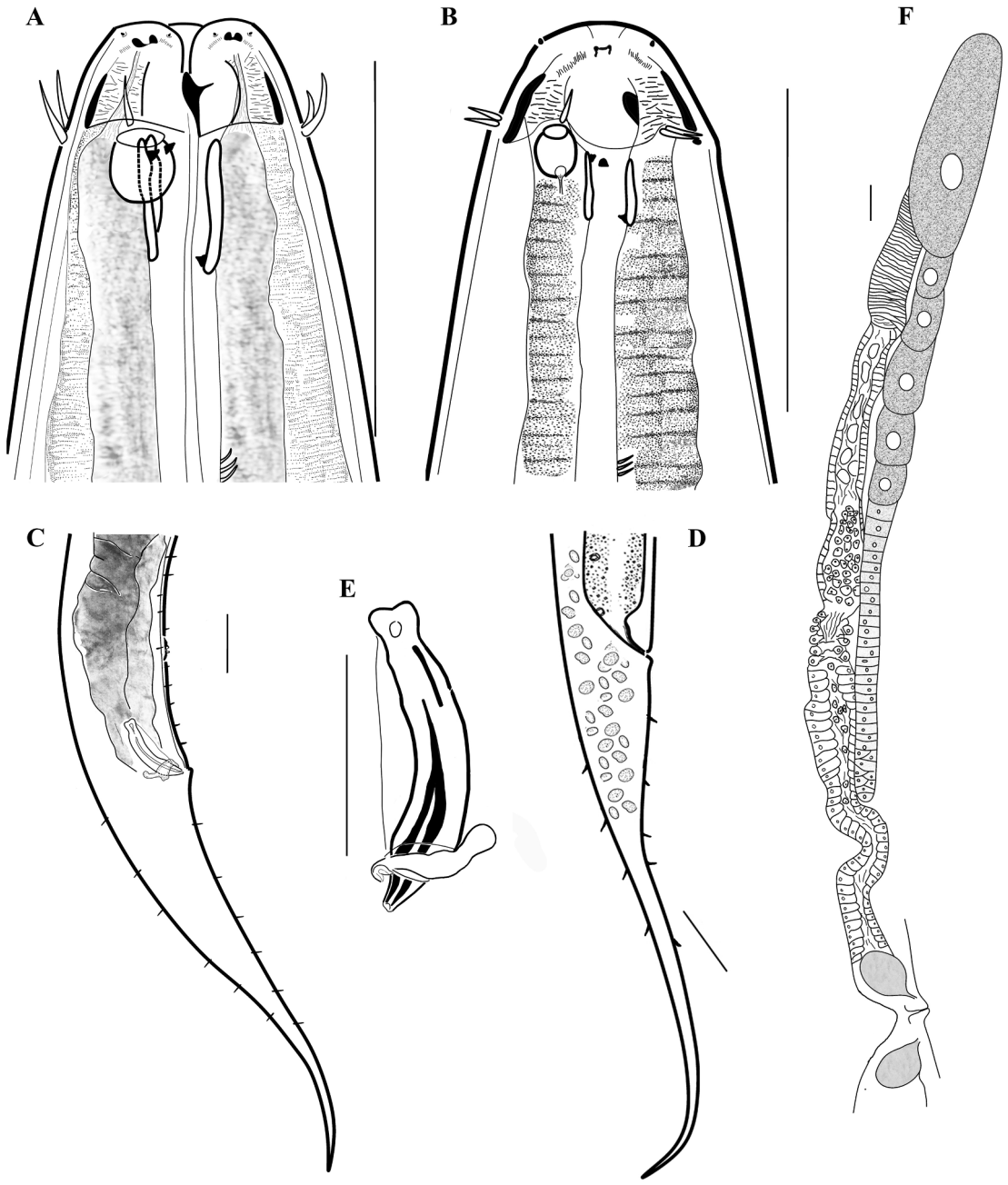

Fig. 11. *Platonova verecunda* sp. nov. (A) Female head. (B) Male head. (C) Male tail. D. Female tail. E. Spicules and gubernaculum, lateral view. F. Female reproductive system, anterior branch. Scale bars: 100 μm.

obtained species with other members of the family Leptosomatidae yielded the following results: *Thoracostoma microlobatum* (FN433817 – FN433818) — 0.260, *Deontostoma* sp. (FN433822 – FN433826) — 0.294, *Thoracostoma trachygaster* (FN433775 – FN433816) – 0.325, *Synonchus* sp. (MG659564) — 0.336, and *Pseudocella* sp. (FN433827 – FN433832) — 0.348. The obtained data indicate a notable divergence between the two new species and the genus *Platonova* in the family Leptosomatidae reported here.

The length of the locus ITS varied among species, with counts of 1280–1281 bp for *P. magna* sp. nov. and 1268 bp for *P. verecunda* sp. nov. The average pairwise K2P distance within each species was 0.005, which is based on nine nucleotide substitutions. Likewise, each ITS sequence relates to a unique haplotype.

P. magna sp. nov. and *P. verecunda* sp. nov. diverged at a 0.140 K2P distance (ITS). This high divergence is based on 160 parsimony-informative sites. In GenBank, only 2 species of Leptosomatidae contain ITS sequences: *Thoracostoma microlobatum* (FN433924) and *T. trachygaster* (FN433917- FN433923). The first species diverged from *P. magna* sp. nov. and *P. verecunda* sp. nov. at 0.364 and 0.357, respectively. The second species varied at 0.394 and 0.403.

3.2.2. Phylogenetic relationships

The total length of the 18S rDNA after assembly and alignment was 1798 bp. Among the members of order Enoplida moderately supported (Bayesian posterior probability, PP = 0.84; Maximum likelihood bootstrap value percent, ML = 35), the primary clade was formed by the family Ironidae, which includes most of the genera identified (*Dolicholaimus, Ironus, Trissonchulus*) (Fig. 18). Bayesian inference (BI) phylogeny revealed a well-supported polytomy node (PP = 0.94), including 7 primary clades of Enoplida nematodes. Tripyloididae (Tripyloidina) was placed as a sister to the clade uniting Trischistomatidae, Trefusiidae and Trischistomatidae (Trefusiina) with moderate support (PP = 0.96; ML = 54). The genus *Syringolaimus* formed a well-supported clade (PP = 1; ML = 99) with *Campydora* and *Rhabdolaimus* (Campydorina). Members of the family Oxystominidae (Ironina) formed three clades and a later branching clade (genus *Halalaimus*) as sister to the Oncholaimina clade. The monophyly of Enoplina was strongly supported (PP = 1), although the basal node was not resolved by BI. Two clades were formed by the genera *Chaetonema* and *Anoplostoma* (Anoplostomatidae), and the third clade included Leptosomatidae, Anticomidae, Enoplidae, Phanodermatidae and Thoracostomatidae. Bayesian analysis did not resolve the Enoplidae and Phanodermatidae groups; however, ML analysis divided these families with moderate support (ML = 52). Maximum likelihood analysis considers Anticomidae as the earliest branching lineage within Enoplina, so the ML and BI topologies differed.

A similar topology with lower support was identified based on the BI of 28S rDNA with a total length after alignment of 786 bp and two members of the order Triplonchida as the outgroup (Fig. 19). The base of the tree constituted a well-supported (PP = 1; ML = 100) politomy node that included 5 primary clades of Enoplia nematodes. The first moderately supported clade (PP = 0.91; ML = 54) united *Alaimus* sp. (Alaimina) and *Syringolaimus* sp. (Campydorina). The second and third clades were strongly supported (PP = 1; ML = 100) and contained members of Oncholaimidae (Oncholaimina) and Tripyloididae (Tripyloidina), respectively. Fourth clade uniting members of Oxystominidae (Ironina) were poorly supported (PP = 0.66; ML = 36); however, further divergence is related to well-supported sister clades (PP = 1; ML = 97–100), including *Oxystomina* sp. and sisters *Thalassoalaimus* sp. and *Litinum* sp. The fifth clade was very poorly supported (PP = 0.57; ML = 24) and contained another member of Ironina – *Dolicholaimus* sp. – rendering that suborder paraphyletic. The sister clade to *Dolicholaimus* sp. was the well-supported (PP = 0.94; ML = 72) monophyletic and moderately resolved group Enoplina. Anoplostomatidae was the earliest branching lineage after which the two sister clades, namely, a strongly supported clade (PP = 1; ML = 100) uniting Enoplidae, Phanodermatidae, and Thoracostomopsidae nematodes and the well supported (PP = 0.99; ML = 81) Leptosomatidae, formed, although the support for this divergence was poor (PP = 0.68; ML = 53). Enoplidae were shown to be paraphyletic, although Phanodermatidae and Thoracostomopsidae were shown to be well-supported (PP = 1; ML = 97–100) monophyletic groups.

The BI phylogeny revealed two well-supported sister clades (PP = 0.88; ML = 72 and PP = 0.99; ML = 80, respectively) of the family Leptosomatidae, one including *Leptosomatides* sp. and *Thoracostoma trachygaster,* and one including the remaining leptosomatids. The earliest branching lineage of the second clade was another species of the genus *Thoracostoma* – *T. microlobatum* – rendering this genus paraphyletic. Further evolution is related to the consecutive divergence of *Deontostoma* (PP = 0.54; ML = 32) and *Pseudocella* (PP = 0.99; ML = 64). The later branching clade united two new species, *Platonova magna* sp.nov. and *P. verecunda* sp.nov., which were well supported (PP = 1; ML = 91), as *Synonchus* sp. (HM564859) and *Platonova verecunda* sp.nov. are in the same clade. The topology of the maximum likelihood tree was congruent with the BI phylogeny in all major clades, although ML analysis resolved the topological issues at the base of the tree with poor support.

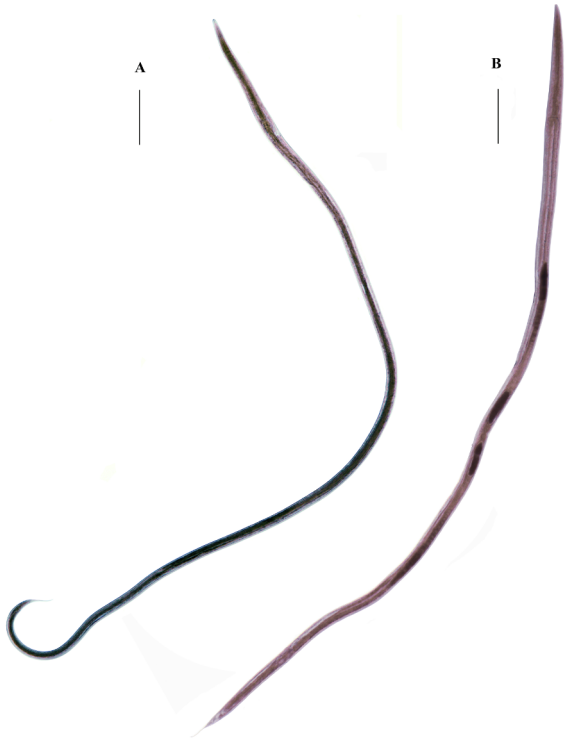

Fig. 12. *Platonova verecunda* sp.nov. Light microscopy. A. Male body. B. Female body. Scale bars: 1000 μm.

The BI phylogeny using COI (399 bp after alignment) did not completely resolve the relationships within the family Leptosomatidae (Fig. 20). *Thoracostoma trachygaster* was the earliest branching lineage and sister to other leptosomatids, but this node was poorly supported (0.52). *Platonova magna* and *P. verecunda* species were sisters to *Thoracostoma microlabatum,* and the received clade was a sister to *Deontostoma*. *Synonchus* was a sister (PP = 0.59) to the clade including apparently different *Pseudocella* species.

4. Discussion

4.1. Morphological analysis

The results of our observations are consistent with data from previous studies, and they confirm the generalizations proposed by Hope (1982) about the structure of the head end of Leptosomatidae, including representatives of Synonchinae. This finding also applies to the structure of the head capsule, the stome armature, and the location of the pharyngeal glands. Two points should be noted. First, the paired protuberances found in the cheilostome of many representatives of Synonchinae seem to be identical to the structures observed for *Platonova*, such as odontia fused with a mandibular ridge. Using a light microscope, this complex looks like a furcate mandible. This complex was described by Platonova (1979) as jaws or forklets. Second, the features of the structure and armature of the pharyngostome that we

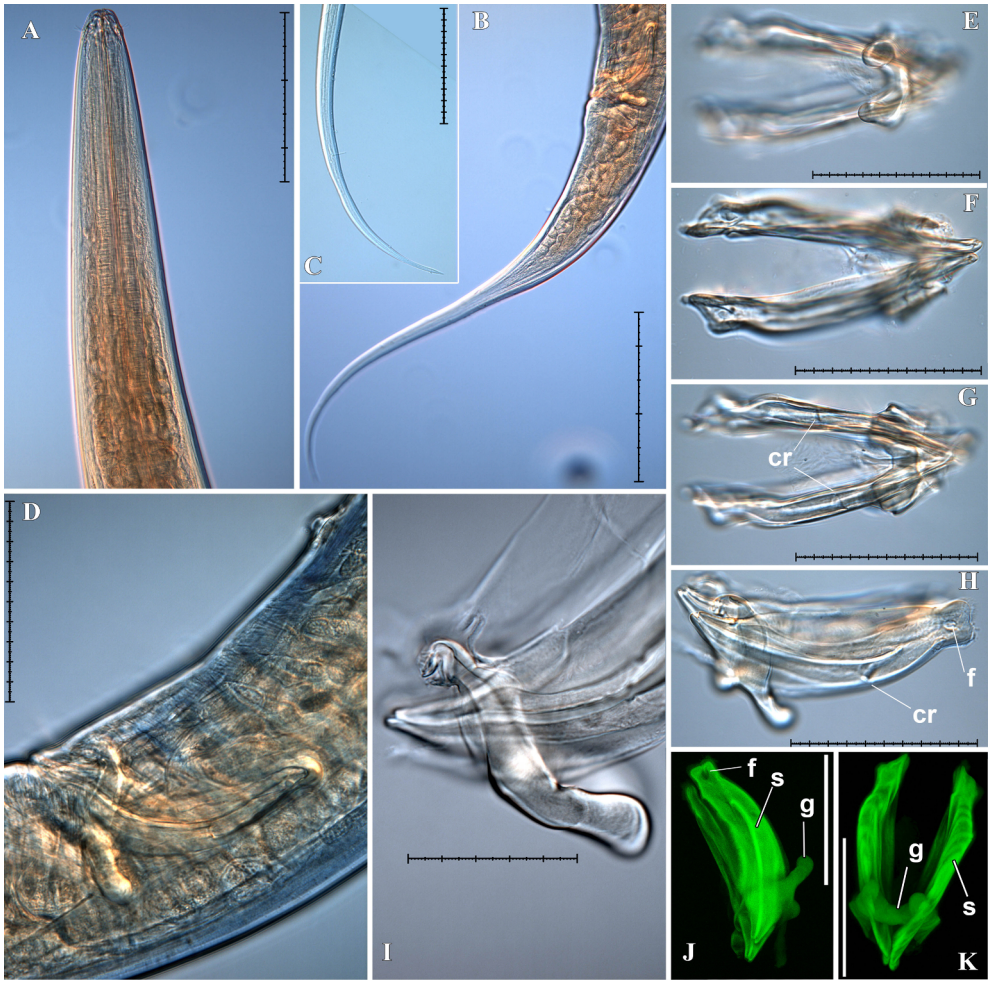

Fig. 13. *Platonova verecunda* sp. nov. A - I light microscopy, DIC. J, K – confocal microscopy. A. Anterior end of the male. B. Posterior end of male. C. Mail tail tip. D. Cloacal region of the male. E - G. Extracted copulatory apparatus of male at different focal planes (dorsal view). H, I. Extracted spicules and gubenaculum, lateral view. J. Spicules and gubernaculum, lateral view. K. Spicules and gubernaculum, dorsal view. Scale bars: A–H, J, K - 100 μm; I - 50 μm. Abbreviations: cr - "crack" on the spicules; f – fenestra; g - gubernaculum; s - spicules.

identified have not been previously described in the literature.

Considerable attention in the identification of nematodes, and in particular Leptosomatidae, is usually given to the structure of the male genital apparatus. However, our research suggests that the interpretation and investigation of the structure of spicules and the gubernaculum using light microscopy require great care due to both the peculiarity of their structure (a large number of elements often superimposed on each other and torsion) and to the significant muscle lining, which makes it difficult to clarify the structure using light microscopy. One of the possible ways to solve this problem is the use of 3D reconstruction, such as with LSCM.

4.2. Molecular analysis

The results of DNA barcoding confirm the validity of the two described species. The average K2P divergence for COI between species was 0.128. According to Derycke et al. (2010a, 2010b), most interspecific congeneric distances for nematodes are within the range of 0.05–0.13; therefore, the described species differ in the upper values of the interspecies distances. High divergence between species was also obtained using ITS, with a K2P distance of 0.140. Thus, the large distances between the species and the results of ABGD analysis confirm the validity of this finding. Interspecific noncogeneric (intergenus) K2P distances for nematodes according to Derycke et al. (2010a, 2010b) are mostly within the range of 0.24–0.63, and the described genus *Platonova* differs from other genera within the family Leptosomatidae, with values from 0.260 to 0.348. Based on the obtained distances, we can argue the validity of the genus *Platonova* when compared to other Leptosomatidae for which sequences are available in GenBank.

The subfamily Leptosomatinae was established by Filipjev (1916) and was long regarded as being within the family Enoplidae (Chitwood and Chitwood, 1950; Clark, 1961; Filipjev, 1934). The accumulation of data on the diversity and structural features of enoplids in general and leptosomatids in particular led to an increase in the rank of the latter to the family Leptosomatidae of the superfamily Enoploidea (de Coninck, 1965; Maggenti, 1981). Platonova (1976) and Andrassy (1976) considered leptosomatids to be a family in the superfamily Leptosomatoidea of the order Enoplida and suborder Enoplina.

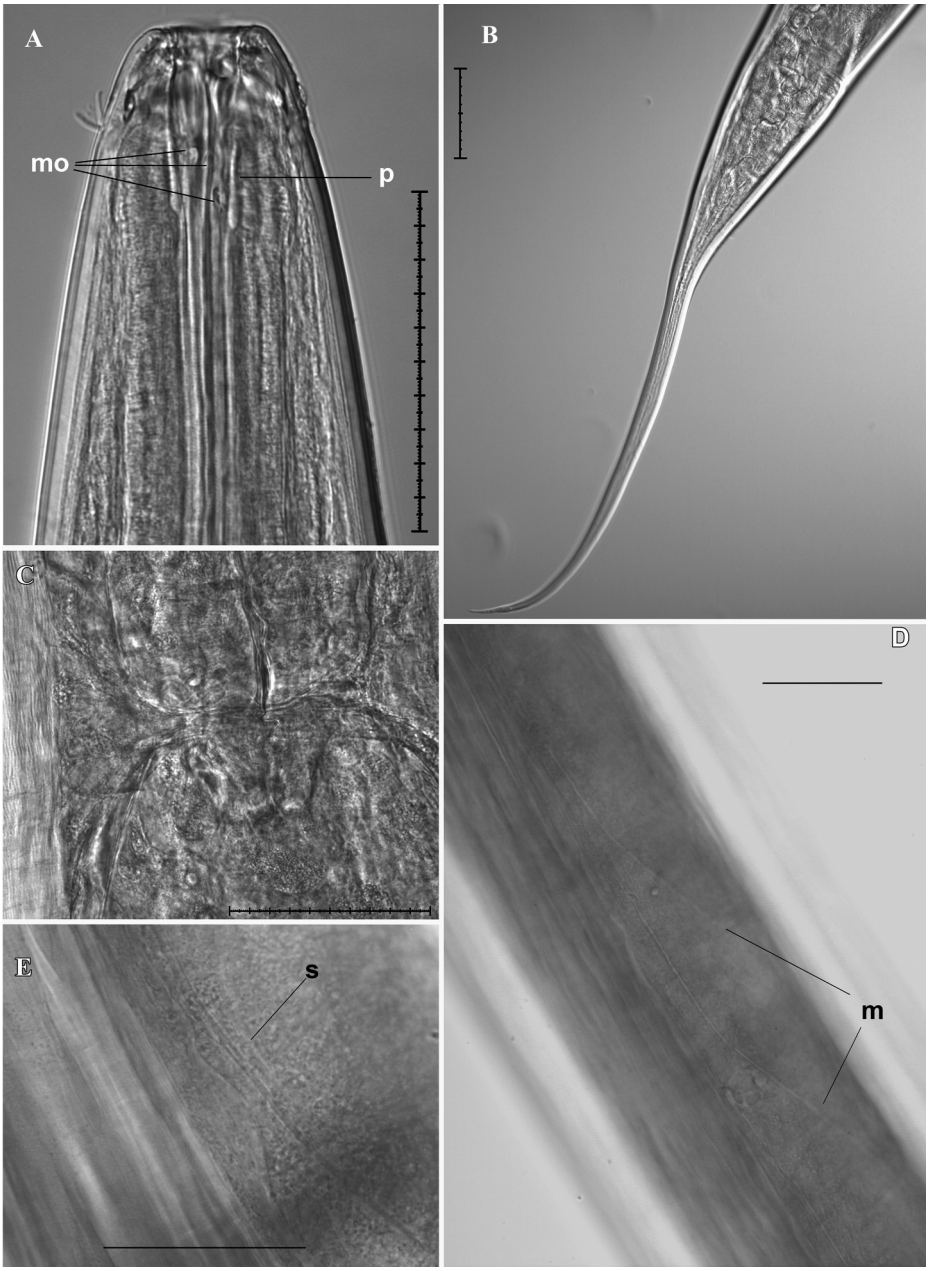

Fig. 14. *Platonova verecunda* sp.nov. Light microscopy. (A) Female anterior end. (B) Female tail. (C) Pharyngeal valve. (D) Lateral epidermal chord with metanemes. (E) Metaneme. Scale bars: 100 μm. Abbreviations: m - metaneme; s - scapulus.

Within Enoplina Lorenzen (1981, 1994) established a new taxon, Enoplacea, including two superfamilies – holophyletic Enoploidea and paraphyletic Ironoidea. The holophyly of the Enoploidea was established (a) by the position of the anterior and posterior gonads to the left of the intestine and (b) by the presence of a single ventrally situated preanal tubule. Additionally, there was no holapomorphy to establish the holophyly of Ironoidea. In this new artificial taxon, Lorenzen included three morphologically different families: Ironidae, Leptosomatidae, and Oxystominidae.

The first molecular studies of the enoplid phylogeny revealed a significantly more complex structure of the order than was assumed based solely on morphological studies. Moreover, these molecular studies were based on a relatively small number of sequences, and for many taxa (including leptosomatids), there was no information. Based on these studies, seven suborders within Enoplida were established instead of 2–3 (De Ley and Blaxter, 2002, 2004). In particular, several Ironidae sequences allowed us to distinguish them from Enoplina and classify them in the independent suborder Ironina. In this way, all representatives of the paraphyletic Ironoidea (including Leptosomatidae), without molecular data, were included in the new suborder.

In recent years, studies on leptosomatids using molecular data have shown the fallacy of this approach. Specimens from Leptosomatidae

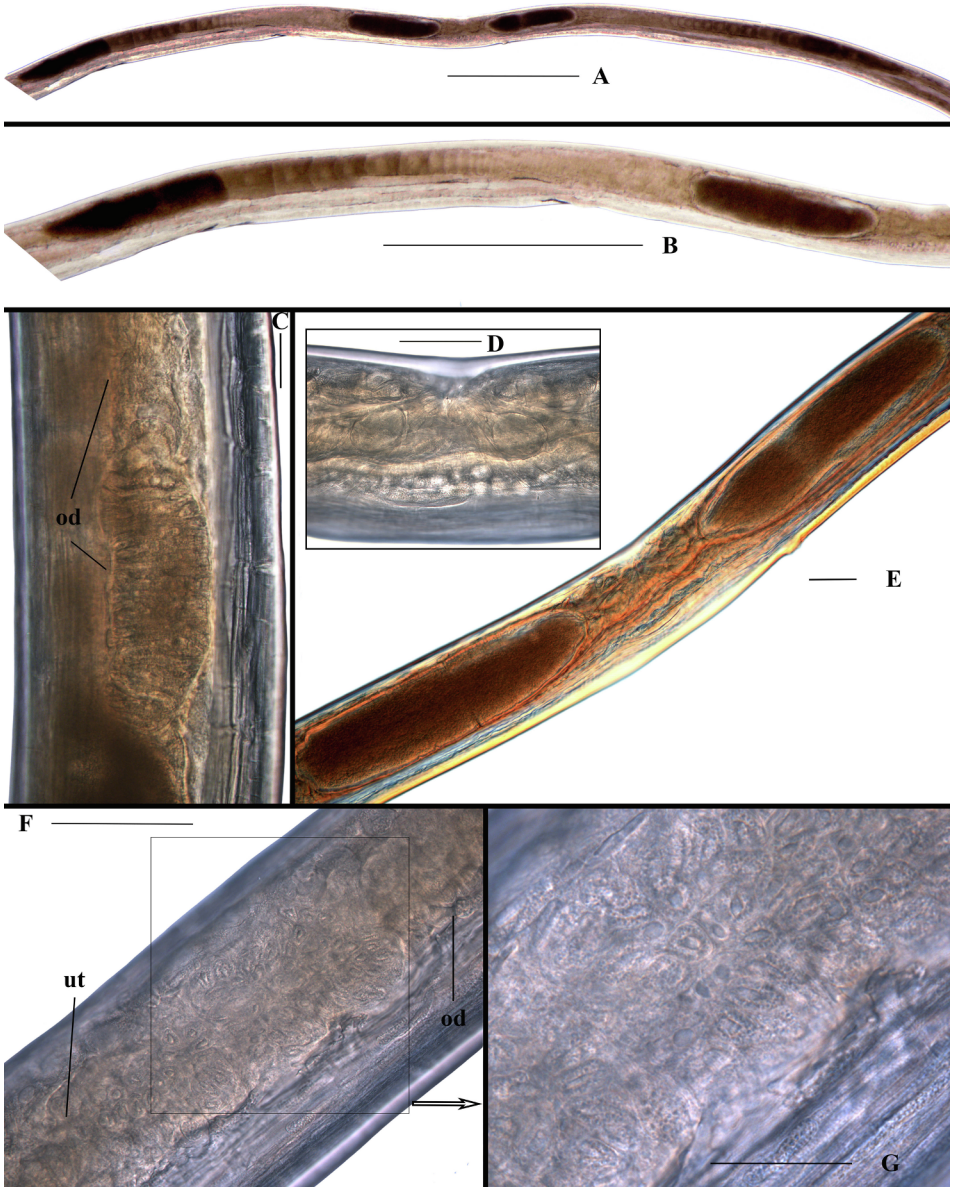

Fig. 15. *Platonova verecunda* sp.nov. Light microscopy. (A) Female reproductive system. (B) Female reproductive system, anterior branch. (C) Narrow part of the oviduct. (D) Vulvar region. (E) Vulvar region and uterus with eggs. (F) Uterus and wider part of the oviduct. (G). Sperm cells in the uterus. Scale bars: A, B - 1000 μm; C, G - 50 μm; D - F - 100 μm. Abbreviations: od - oviduct; ut - uterus.

were always recovered within a single clade with high support (100% bootstrap support in ML and posterior probabilities of 0.99 in Bayesian trees), together with the families belonging to Enoploidea (Bik et al., 2010a, 2010b; Smythe, 2015). Despite these results, in all modern classifications of Enoplida, leptosomatids are still considered within the suborder Ironina (Bezerra et al., 2019; Smol et al., 2014).

Our study confirms the results of Bik et al. (2010a, 2010b) and Smythe (2015); notably, despite the increasing number of 18 rDNA sequences of nematodes, Bayesian and maximum likelihood phylogenetic trees had a similar topology. In each case, the members of the family Anoplostomatidae were placed at the base of two clades: the monophyletic Leptosomatidae and the clade containing the remaining Enoplinae, including Anticomidae, Enoplidae, Thoracostomopsidae and Phanodermatidae. Notably, Anoplostomatidae appears to be polyphyletic, as the genus *Anoplostoma* shows an early branching clade within Enoploidea, and the genus *Chaetonema* occupies a lower position (Bik et al., 2010a, 2010b; Smythe, 2015, Fig. 19). The BI approach reveals that *Anticoma* sp. occupies a lower position than leptosomatids. Despite the missing data in many groups of nematodes (e.g., *Anoplostoma*, *Anticoma* and some genera of Thoracostomopsidae), the phylogenies based on 28S and on 18S are similar in topology. The topological tree supports the basal positions of Anoplostomatidae and the suborder Enoplina, including Leptosomatidae.

We also obtained a strongly supported clade that included *Campydora*, *Rhabdolaimus* and *Syringolaimus*. This finding confirms the latest results of the revision of the suborder Campydorina (Holovachov,

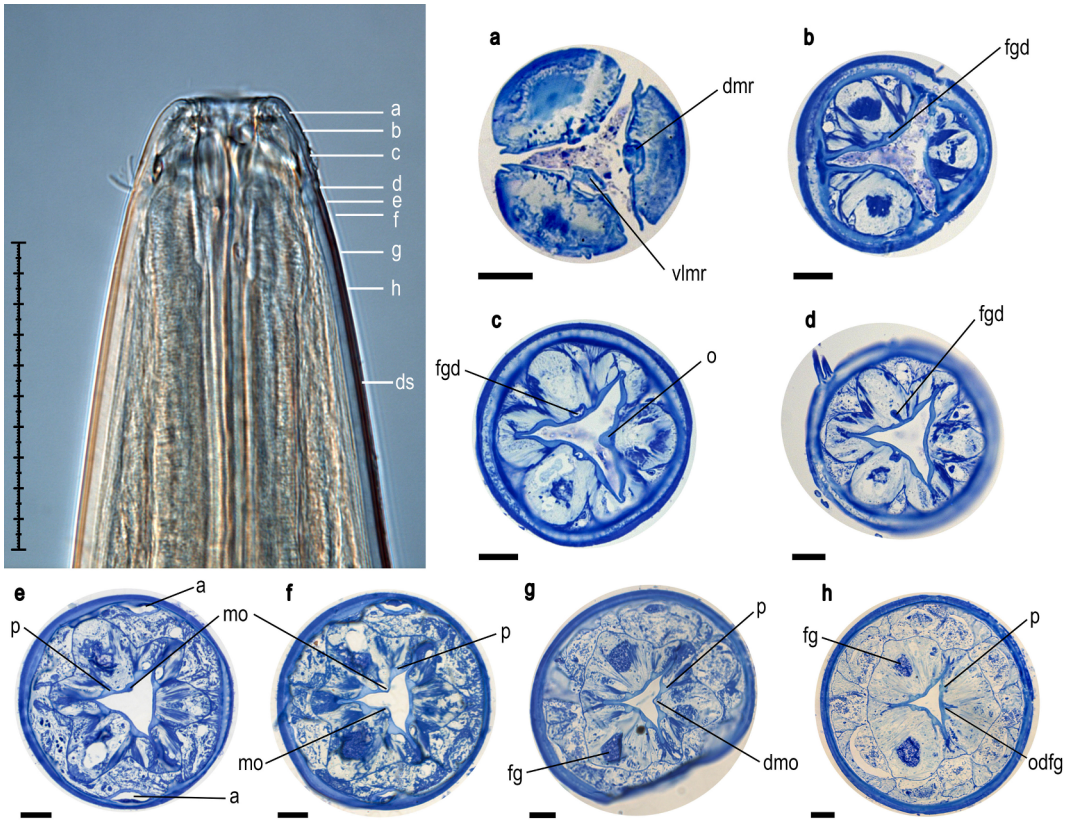

Fig. 16. *Platonova verecunda* sp. nov. Anterior end of the female showing levels of sectioning (scale bar - 100 μm). Light microphotographs of transverse sections. Dorsal to the right. a. Mouth opening at the level of mandibular ridges. b. Buccal cavity at the level of pharyngeal gland ducts. c. Buccal cavity at the level of dorsal onchium. d. Buccal cavity at the level of head setae. e. Buccal cavity ant the level of amphids and ventrosublateral microonchium. f. Buccal cavity at the level of ventrosublateral macronchia and cuticular beams. g. Buccal cavity and the level of dorsal microonchium. h. Posterior part of the buccal cavity. Scale bars: 10 μm. Abbreviations: a – amphid; dmr – dorsal mandibular ridge; dmo – dorsal microonchium; ds – dorsal side; fg – pharyngeal glands; fgd – pharyngeal gland ducts; mo – microonchium; o – dorsal onchium; odfg - orifice of the dorsal pharyngeal gland; p – cuticular beams.

2019). Additionally, we have observed some new features in the topological tree. In particular, Oxystominidae formed three clades instead of two (Bik et al., 2010a, 2010b; Smythe, 2015), and the *Halalaimus* clade was as sister to Oncholaimina. Moreover, according to Bik et al. (2010a, 2010b) and Smythe (2015), Ironidae is a sister to Alaimina. In our study, the members of the family Ironidae were placed as the earliest branching lineage within Enoplida. However, this topology was poorly supported (PP = 0.84; ML = 35) and possibly related to the addition of *Trissonchulus* in the analysis. Therefore, Clade 2, including Alaimidae and Ironidae recovered by Bik et al. (2010a, 2010b), did not maintain monophyly. Furthermore, according to the 28S trees, the *Dolicholaimus* sp. forms a sister relationship with Enoplina with poor support. Thus, BI and ML phylogenetic analyses based on 18S and 28S rDNA suggest that Leptosomatidae requires a transfer from the superfamily Ironoidea (suborder Ironina) to superfamily Enoploidea (suborder Enoplina).

The phylogenetic relationships within the family Leptosomatidae remained unresolved despite the various sequences obtained for different loci. Most sequences of leptosomatids obtained were from COI. Derycke and co-authors (Derycke et al., 2005, 2010a) considered *Thoracostoma trachygaster* as basal splits within Leptosomatidae. Apparently different species of the genera *Pseudocella* and *Deontostoma* occupy low positions, and *Thoracostoma microlabatum* is included as a sister to the *Deontostoma* clade. The Bayesian tree fully confirms this topology, although the support of most nodes was low (Fig. 20). In this study, we used Anoplostomatidae as an outgroup. Both *Platonova* species were sisters to *Thoracostoma microlabatum* and the receiving sister to the *Deontostoma* clade. The genus *Synonchus* was a sister to the clade *Pseudocella*, which apparently included three species. The phylogenetic tree based on 28S rDNA shows a different topology (Fig. 19). *Platonova* was a sister to *Pseudocella* and *Deontostoma,* and it occupied a relatively basal position. *Thoracostoma microlabatum* occupied a separate position as *Platonova, Pseudocella* and *Deontostoma.* Moreover, other species of the genus *Thoracostoma* (*T. trachygaster, T. igniferum,* and *T. fatimae*) formed early branching Enoplida lineages, the same pattern as observed in the COI-based phylogeny. *Leptosomatides* also have a basal position according to Smythe (2015). Finally, the phylogeny based on 18S rDNA placed *Proplatycoma fleurdelis* as the basal node to other leptosomatids, in contrast with the findings of Smythe (2015). Nevertheless, the relationships among the rest of the members Leptosomatidae were unresolved and poorly supported. It is important to note that the specimen *Synonchus* sp. TCR206 is extremely similar to *Platonova verecunda* for 18S and 28S rDNA. Therefore, we consider it necessary to transfer the TCR206 sequence from *Synonchus* to *Platonova verecunda* sp. nov.

4.3. Spatial distribution

Within the study area, both described species were found only in the

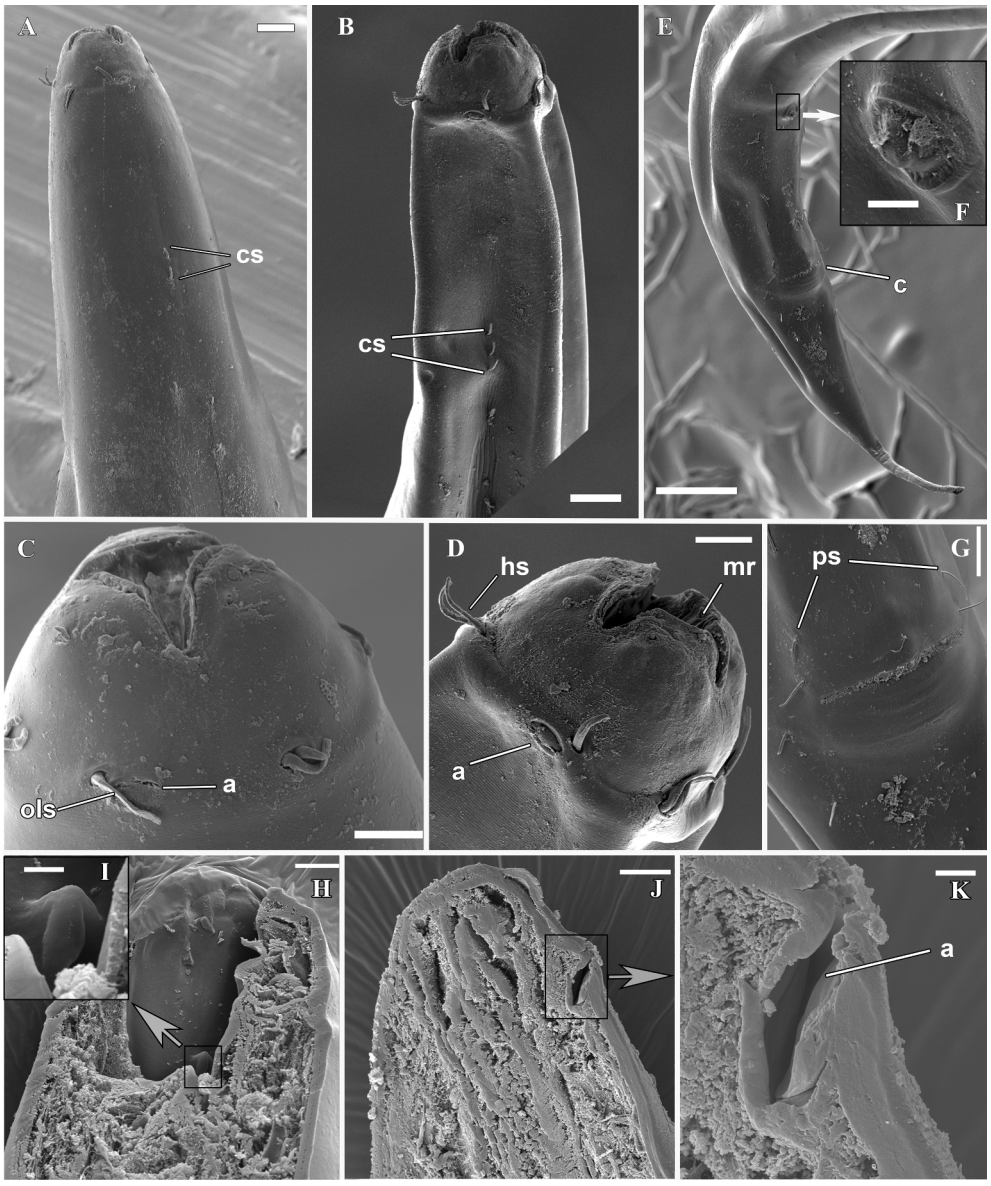

Fig. 17. *Platonova verecunda* sp. nov. Scanning electron microscopy. (A) Anterior end of female, lateral view. (B) Anterior end of male, lateral view. (C) Head of female, lateral view. (D) Head of male, lateral view. (E) Posterior end of male, ventral view. (F) Supplementary organ. (G) Pericloacal region of male, ventral view. (H) Longitudinal section through the buccal cavity. (I) Microonchium. (J, K) Longitudinal section through the amphid. Scale bars: A, B, G - 20 μm; C, D, F, H, J - 10 μm; I, K - 2 μm; E - 100 μm. Abbreviations: a - amphid; c - cloacal opening; cs - cervical setae; hs - head setae; mr – mandibular ridge; ols - outer labial setae; ps - precloacal setae; sup - supplementary organ.

Kuril-Kamchatka Trench and adjacent water areas, and they were absent in the Sea of Okhotsk and the Sea of Japan. In addition, these species exhibited different spatial distribution patterns. *P. magna* sp. nov. was only found at abyssal depths on both sides of the trench. In contrast, *P. verecunda* sp. nov. was found within the trench, up to the greatest depths recorded. In addition, a sample of almost identical *P. verecunda* sp. nov. was obtained off the coast of California at a depth of 2695 m (Bik et al., 2010a, 2010b). High similarity between the sequences on both sides of the Pacific Ocean may indicate the absence of barriers and high connectivity. Thus, 1) in spite of the absence of a pelagic stage of development in their life cycle, deep-sea nematodes can potentially be characterized by an extremely wide spatial distribution (in our case, an *amphi*-Pacific distribution); 2) for the described species, the deep-sea trench is not considered a barrier to dispersal; and 3) the vertical range of distribution for some species may be more than 6500 m. However, the lack of species in the Sea of Okhotsk and the Sea of Japan may indicate the impossibility of overcoming straits with relatively shallow depths.

5. Concluding remarks

Our results demonstrate the high diversity of marine nematodes, which has been rarely studied. Despite the relatively simple general morphological structure, the corresponding individual morphological elements (in particular, the feeding apparatus structure and copulatory apparatus) are extremely diverse. Additionally, the implementation of an integrated approach that combines various methods of morphological analysis, information technology, and the use of molecular methods to study marine nematodes is of particular importance. Such an approach can provide an adequate understanding of the structure, phylogenetics, and biogeography of nematodes. It should be noted that a very small number of nucleotide sequences are available for leptosomatids. Of the 32 genera of Leptosomatidae, represented by 185 species (Bezerra et al., 2019), only sequences of 9 genera could be found in databases. Therefore, the phylogenetic relationships within Leptosomatidae can only be resolved by increasing the available molecular data. An increase in the availability of such information will

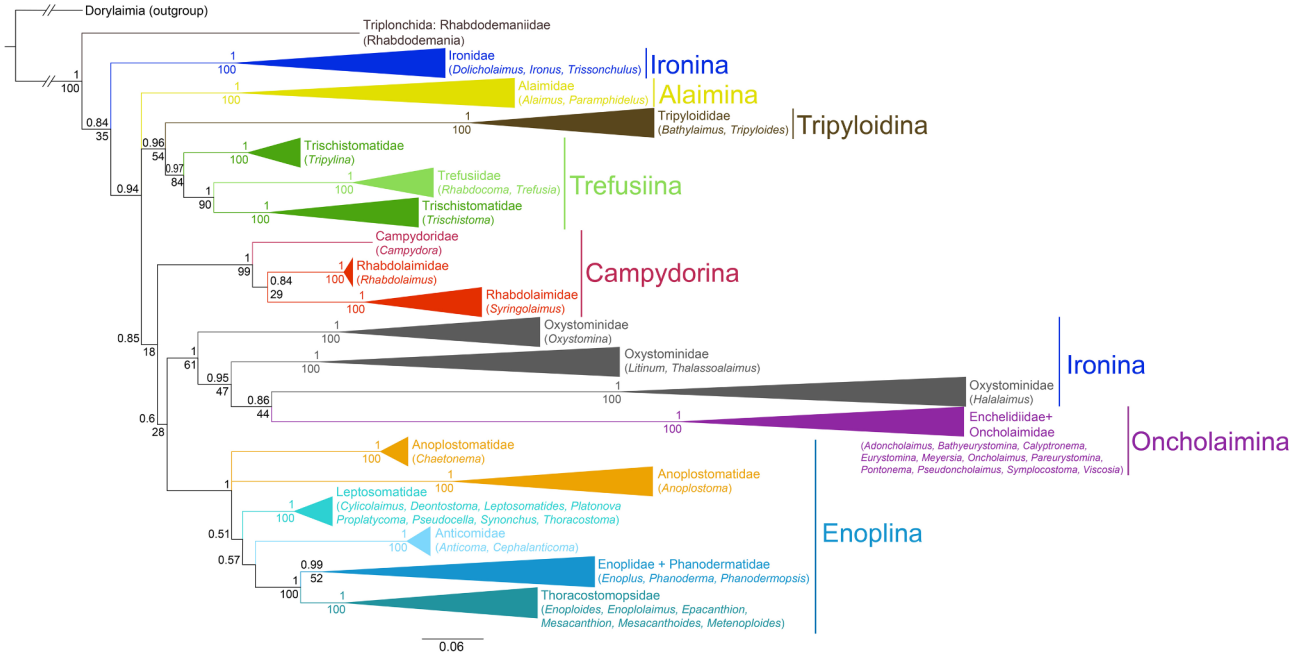

Fig. 18. Bayesian 18S rDNA phylogeny of the order Enoplida from 383 taxa, using the GTR + I + G model of nucleotide substitution. *Allodorylaimus* (Dorylaimida) and some members of Triplonchida were used as outgroup to root the tree. Bayesian posterior probabilities (PP) are given above tree nodes and bootstrap support values found in the ML analysis are shown below nodes.

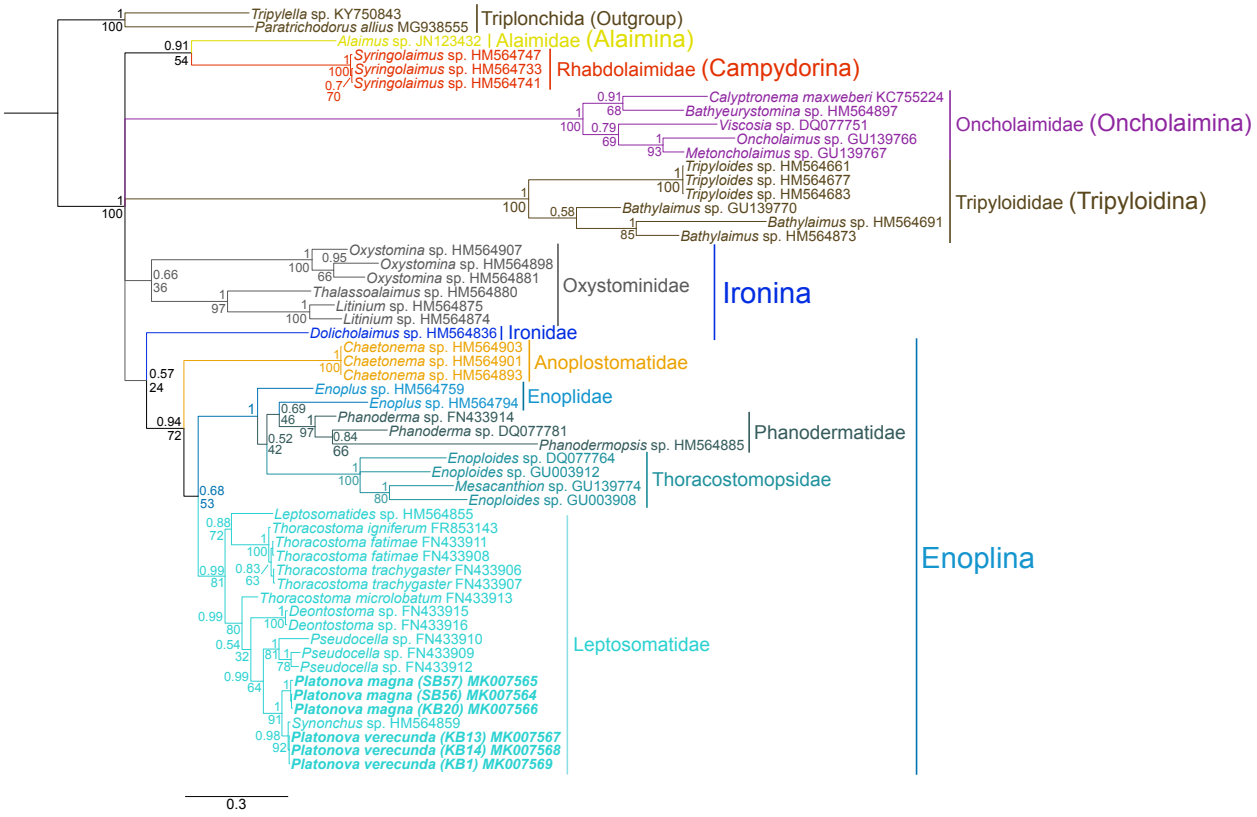

Fig. 19. Bayesian 28S rDNA phylogeny of the order Enoplida from 55 taxa, using the GTR + I + G model of nucleotide substitution. *Paratrichodorus allius* and *Tripylella* (Triplonchida) were used as outgroup to root the tree. Specimens obtained in this study are in bold.

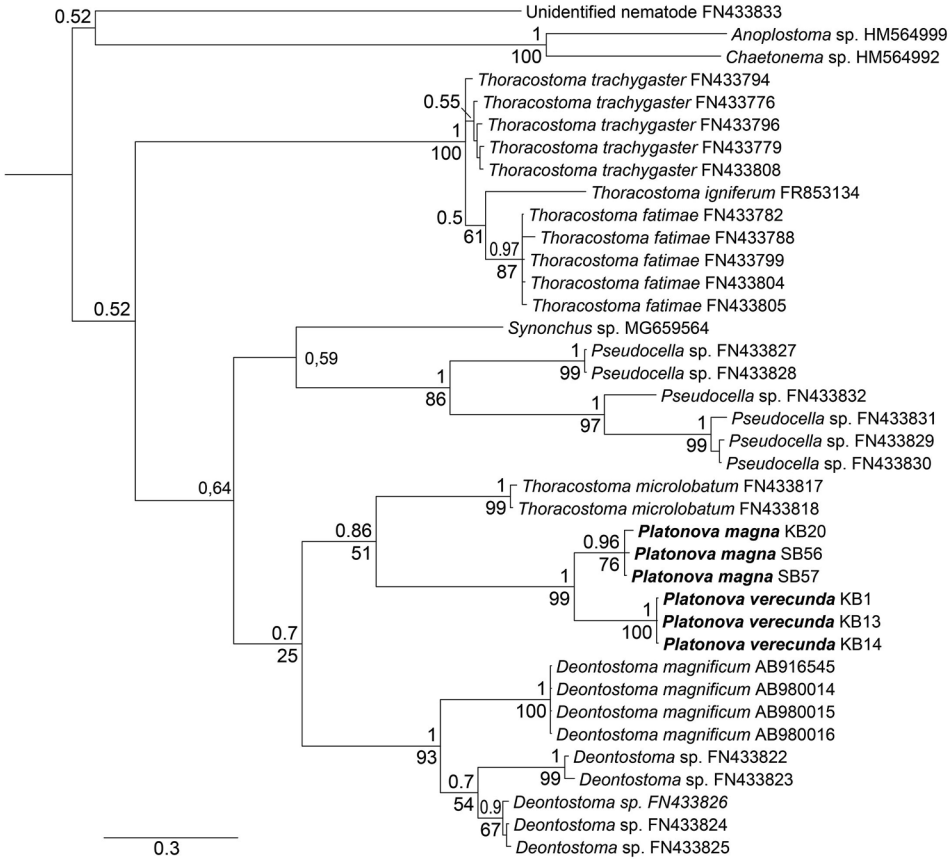

Fig. 20. Bayesian mitochondrial COI phylogeny of the family Leptosomatidae from 38 taxa, using the HKY + I + G model of nucleotide substitution for first and third codon position and F81 + G for second position. *Anoplostoma* and *Chaetonema* (Anoplostomatidae) were used as outgroup to root the tree. Specimens obtained in this study are in bold.

offer further insights into studies of the spatial distribution of nematodes. Moreover, the position of Leptosomatidae within Enoplida can be resolved.

Acknowledgements

The material was collected and sorted within the framework of several large international projects. The KuramBio I and II projects were financially supported by the PTJ (German Ministry for Science and Education), grant 03G0857A, KuramBio I BMBF grant 03G0223A, as well as KuramBio II BMBF grant 03G0250A to Prof. Dr. Angelika Brandt, University of Hamburg, now Senckenberg Museum, Frankfurt, Germany. Sampling and preliminary processing was partially supported by the Russian Science Foundation (agreement no. 14-50-00034), Russian Federation Government grant No 11.G34.31.0010. The scanning electron microscopy investigations were done in the A.V. Zhirmunsky National Scientific Centre of Marine Biology FEB RAS. The authors are grateful to D.V. Fomin for technical assistance for the SEM facilities of the Far East Center of Electron Microscopy. The light microscopy investigation and molecular analyses were done in the Far Eastern Federal University and were financially supported by FEFU through grant award no. D-38-19.

We are very grateful to Prof. Dr. A. Brandt (Senckenberg Research Institute and Natural History Museum, and Goethe University Frankfurt, Frankfurt) and to Dr. M.V. Malyutina (NSCMB FEB RAS) for invitation to join international projects and the deep-sea expeditions; to anonymous reviewers for the constructive comments and suggestions, which have considerably improved the manuscript. We thank the crews of the RVs Sonne and Akademik M.A. Lavrentyev for their help on board and all student helpers and technicians for their assisting during expeditions. This is KuramBio II publication # 50.

References

Andrassy, I., 1976. Evolution as a Basis for the Systematization of Nematodes. Pitman Publishing, London - San Francisco - Melbourne, pp. 288.

Bezerra, T.N., Decraemer, W., Eisendle-Flöckner, U., Hodda, M., Holovachov, O., Leduc, D., Miljutin, D., Mokievsky, V., Peña Santiago, R., Sharma, J., Smol, N., Tchesunov, A., Venekey, V., Zhao, Z., Vanreusel, A., 2019. Nemys: World Database of Nematodes. http://nemys.ugent.be on 2019-05-15. https://doi.org/10.14284/366.

Bik, H.M., Lambshead, P.J.D., Thomas, W.K., Hunt, D.H., 2010a. Moving towards a complete molecular framework on the Nematoda: a focus on the Enoplida and early-branching clades. BMC Evol. Biol. 10, 353.

Bik, H.M., Thomas, W.K., Lunt, D.H., Lambshead, P.J.D., 2010b. Low endemism, continued deep-shallow interchanges, and evidence for cosmopolitan distributions in free-living marine nematodes (order Enoplida). BMC Evol. Biol. 10, 389.

Blaxter, M.L., De Ley, P., Garey, J.R., Liu, L.X., Scheldeman, P., Vierstraete, A., Vanfleteren, J.R., Mackey, L.Y., Dorris, M., Frisse, L.M., Vida, J.T., Thomas, W.K., 1998. A molecular evolutionary framework for the phylum Nematoda. Nature 392, 71–75.

Bowles, J., Blair, D., McManus, D.P., 1992. Genetic variants within the genus Echinococcus identified by mitochondrial DNA sequencing. Mol. Biochem. Parasitol. 54, 165–174.

Brandt, A., Elsner, N., Brenke, N., Golovan, O.A., Lavrenteva, A.V., Malyutina, M.V., Riehl, T., 2015. Abyssal macrofauna of the Kuril-Kamchatka Trench area collected by means of a camera-epibenthic sledge (Northwest Pacific). Deep-Sea Res. II 111, 175–188.

Chitwood, B.G., Chitwood, M.B., 1950. An Introduction to Nematology. Monumental Printing, Baltimore, pp. 213.

Clark, W.C., 1961. A revised classification of the order Enophda (Nematoda). N. Z. J. Sci. 4, 123–150.

De Coninck, L.A. (1965). Classe des Nématodes: Systematique des nématodes et sous-classe des Adenophorea. In: Grassé, P.P. (Ed.) Traité de Zoologie, vol. 4, pp. 586–681.

De Grisse, A.T., 1969. Redescription ou modifications de quelques techniques utilisees dans l'etude des nematodes phytoparasitaires. Mededelingen Rijksfakultiet Landbouwwetenschappen Gent 34, 352–369.

De Ley, P., Blaxter, M., 2002. Systematic position and phylogeny. In: Lee, D. (Ed.), The Biology of Nematodes. Harwood Academic Publishers, Reading, pp. 1–30.

De Ley, P., Blaxter, M.L., 2004. A new system for Nematoda: combining morphological characters with molecular trees, and translating clades into ranks and taxa. Nematol. Monogr. Persp. 2, 633–653.

De Oliveira, D.A.S., Decraemer, W., Holovachov, O., Burr, J., De Ley, I.T., De Ley, P., et al., 2012. An integrative approach to characterize cryptic species in the *Thoracostoma trachygaster* Hope, 1967 complex (Nematoda: Leptosomatidae). Zool. J. Linn. Soc. 164 (1), 18–35.

Derycke, S., De Ley, P., De Ley, I.T., Holovachov, O., Rigaux, A., Moens, T., 2010a. Linking DNA sequences to morphology: cryptic diversity and population genetic structure in the marine nematode *Thoracostoma trachygaster* (Nematoda, Leptosomatidae). Zool. Scr. 39, 276–289.
Derycke, S., Remerie, T., Vierstraete, A., Backeljau, T., Vanfleteren, J., et al., 2005. Mitochondrial DNA variation and cryptic speciation within the free-living marine nematode *Pellioditis marina*. Mar. Ecol. Prog. Ser. 300, 91–103.
Derycke, S., Vanaverbeke, J., Rigaux, A., Backeljau, T., Moens, T., 2010b. Exploring the use of cytochrome oxidase c subunit 1 (COI) for DNA barcoding of free-living marine nematodes. PloS One 5, e13716.
Fadeeva, N.P., Zograf, J.K., 2010. New and known species of *Enoplolaimus* (Enoplida: Thoracostomopsidae) from the Sea of Japan. Nematology 12 (5), 731–749.
Felsenstein, J., 1981. Evolutionary trees from DNA sequences: a maximum likelihood approach. J. Mol. Evol. 17, 368–376.
Filipjev, I.N., 1916. Free living nematodes in the collection of the Zoological Museum of the Imperial Academy of Sciences in Petrograd. Ezheg. zool. Muz Petrograd. 21, 59–116.
Filipjev, I.N., 1934. The classification of the free-living nematodes and their relation to the parasitic nematodes. Smithson. Misc. Collect. 89, 1–63.
Fonseca, G., Derycke, S., Moens, T., 2008. Integrative taxonomy in two free-living nematode species complexes. Biol. J. Linn. Soc. 94, 737–753.
Gunton, L.M., Bett, B.J., Gooday, A.J., Glover, A.G., Vanreusel, A., 2017. Macrofaunal nematodes of the deep Whittard Canyon (NE Atlantic): assemblage characteristics and comparison with polychaetes. Mar. Ecol. 38 (2), e12408.
Hasegawa, M., Kishino, H., Yano, T., 1985. Dating the human-ape splitting by a molecular clock of mitochondrial DNA. J. Mol. Evol. 22, 160–174.
Holovachov, O., 2019. *Campydoroides manautei* gen. et sp. nov. from New Caledonia and a reappraisal of the suborder Campydorina (Nematoda). Eur. J. Taxonomy 518, 1–23.
Hope, W.D., 1982. Structure of head and stoma in the marine nematode genus Deontostoma (Enoplida: Leptosomatidae). Smithsonian Contrib. Zool. 353, 1–22.
Kumar, S., Stecher, G., Tamura, K., 2016. MEGA7: Molecular Evolutionary Genetics Analysis version 7.0 for bigger datasets. Mol. Biol. Evol. 33 (7), 1870–1874.
Lanfear, R., Calcott, B., Ho, S.Y., Guindon, S., 2012. Partitionfinder: combined selection of partitioning schemes and substitution models for phylogenetic analyses. Mol. Biol. Evol. 29, 1695–1701.
Leduc, D., Zhao, Z., 2016. Phylogenetic relationships within the superfamily Desmodoroidea (Nematoda: Desmodorida), with descriptions of two new and one known species. Zool. J. Linn. Soc. 176 (3), 511–536.
Leduc, D., Zhao, Z.Q., 2019. Morphological and molecular characterisation of *Spirinia antipodea* Leduc n. sp. (Nematoda: Desmodoridae), a cryptic species related to *S. parasitifera*, from the coast of New Zealand. Nematology. 21 (1), 91–105.
Lorenzen, S., 1981. Entwurf eines phylogenetischen systems der freilebenden nematoden. Vero¨ffentlichungen des Institut für Meeresforschungen in Bremerhaven 7, 1–472.
Lorenzen, S., 1994. The Phylogenetic Systematics of Free-Living Nematodes. The Ray Society, London.
Maggenti, A.R., 1981. General Nematology. Springer-Verlag, New York.
Meldal, B.H.M., Debenham, N.J., De Ley, P., De Ley, I.T., Vanfleteren, J.R., Vierstraete, A.R., Bert, W., Borgonie, G., Moens, T., Tyler, P.A., Austen, M.C., Blaxter, M.L., Rogers, A.D., Lambshead, P.J.D., 2007. An improved molecular phylogeny of the Nematoda with special emphasis on marine taxa. Mol. Phylogenet. Evol. 42, 622–636.
Nunn, G.B., 1992. Nematode molecular evolution. Ph.D. Thesis. University of Nottingham, UK.
Platonova, T.A., 1970. On the Taxonomy of the Leptosomatidae (Nematoda) of the Mediterranean Sea and of the Adjacent Waters of the Atlantic [O sistematike Leptosomatidae (Nematoda) Sredizemnogo Morya i prilezhashchikh vod Atlantiki]. Zoologicheskii Zhurnal 49 (9), 1298–1305.
Platonova, T.A., 1976. Lower Enoplida (free-living marine nematodes) of the seas of the USSR (in Russian). Issledovaniya Fauny Morei (Nematody i ikh rol' v meiobentose) 15(23), 3–164.
Platonova, T.A., 1979. Structure of the head end and system of the subfamily Synonchinae (Nematoda, Enoplida, Leptosomatidae) (Struktura golovnogo kontsa i sistema podsemeistva Synonchinae (Nematoda, Enoplida, Leptosomatidae)). Zoologicheskii Zhurnal 58 (8), 1117–1129.
Puillandre, N., Lambert, A., Brouillet, S., Achaz, G., 2012. ABGD, Automatic Barcode Gap Discovery for primary species delimitation. Mol. Ecol. 21, 1864–1877.
Rambaut, A., Drummond, A.J., Xie, D., Baele, G., Suchard, M.A., 2018. Posterior summarisation in Bayesian phylogenetics using Tracer 1.7. Syst. Biol. 67 (5), 901–904.
Ronquist, F., Huelsenbeck, J.P., 2003. MrBayes 3: Bayesian phylogenetic inference under mixed models. Bioinformatics 19, 1572–1574.
Seinhorst, J.W., 1959. A rapid method for the transfer of nematodes from fixative to anhydrous glycerin. Nematologica 4, 67–69.
Sharma, J., Baguley, J.G., Bluhm, B.A., Rowe, G.T., 2011. Do Meio- and Macrobenthic nematodes differ in community composition and body weight trends with depth? PLoS ONE 6 (1), e14491.
Smol, N., Muthumbi, A., Sharma, J., 2014. Order Enoplida. In: Schmidt-Rhaesa, A. (Ed.), Handbook of Zoology. Gastrotricha, Cycloneuralia, Gnathifera. Vol. 2. Nematoda. de Gruyter, Berlin, pp. 193–249.
Smythe, A.B., 2015. Evolution of feeding structures in the marine nematode order Enoplida. Integr. Comp. Biol. 55 (2), 228–240.
Stamatakis, A., 2006. RAxML-VI-HPC: maximum likelihood-based phylogenetic analyses with thousands of taxa and mixed models. Bioinformatics 22, 2688–2690.
Tavaré, S., 1986. Some probabilistic and statistical problems in the analysis of DNA sequences. In: Miura, R.M. (Ed.), Some Mathematical Questions in Biology – DNA Sequence Analysis. Amer Math Soc, Providence, RI, pp. 57–86.
Tchesunov, A.V., 2006. Biology of Marine Nematodes. KMK Scientific Press Ltd, Moscow, pp. 367.
Truett, G.E., Heeger, P., Mynatt, R.L., Truett, A.A., Walker, J.A., Warman, M.L., 2000. Preparation of PCR-quality mouse genomic DNA with hot sodium hydroxide and tris (HotSHOT). Biotechniques 29, 52–54.
Vrain, T.C., Wakarchuk, D.A., Levesque, A.C., Hamilton, R.I., 1992. Intraspecific rDNA restriction fragment length polymorphism in the *Xiphinema americanum* group. Fund. Appl. Nematol. 15, 563–573.
Wallace, I.M., O'Sullivan, O., Higgins, D.G., Notredame, C., 2006. M-Coffee: combining multiple sequence alignment methods with T-Coffee. Nucl. Acids Res. 34 (6), 1692–1699.
Warwick, R.M., 1973. Freeliving marine nematodes from the Indian Ocean. Bull. Br. Mus. Nat. Hist. (Zool.) 25 (3), 85–117.
Zullini, A., Villa, A.M., 2006. Redescription of three tobrilids (Nematoda) from Altherr's collection using confocal microscopy. J. Nematode Morphol. System. 8, 121–132.